Intraseasonal Variability

- Understanding the climate variability associated with Intraseasonal Oscillation

Prediction Research Team
Ja-Yeon Moon

APCC
APEC CLIMATE CENTER

APCC in the Forefront of S2S Forecast:

Leading the way in the fight against extreme phenomena

1 Intraseasonal Oscillation

2 Seasonal dependence

3 Interannual variability

4 Teleconnection

APCC
APEC CLIMATE CENTER

1. Intraseasonal oscillation

- Basics

Intraseasonal oscillation

ISO ? Variability on timescales of 20-100 days, timescale between the typical weather (up to 15 days) and climate (from a season and beyond).
The importance of the tropical ISO to bridge weather and climate has been increasingly recognized.

Distinctions among different terminologies to describe tropical atmospheric variability on the intraseasonal timescales,
It is of little doubt that there are two dominant components.
One is eastward propagating component, which commonly referred to as the MJO, the other is a northward propagating component associated with the Asian summer monsoon, BSISO.

Ref. Chidong Zhang

Madden-Julian Oscillation

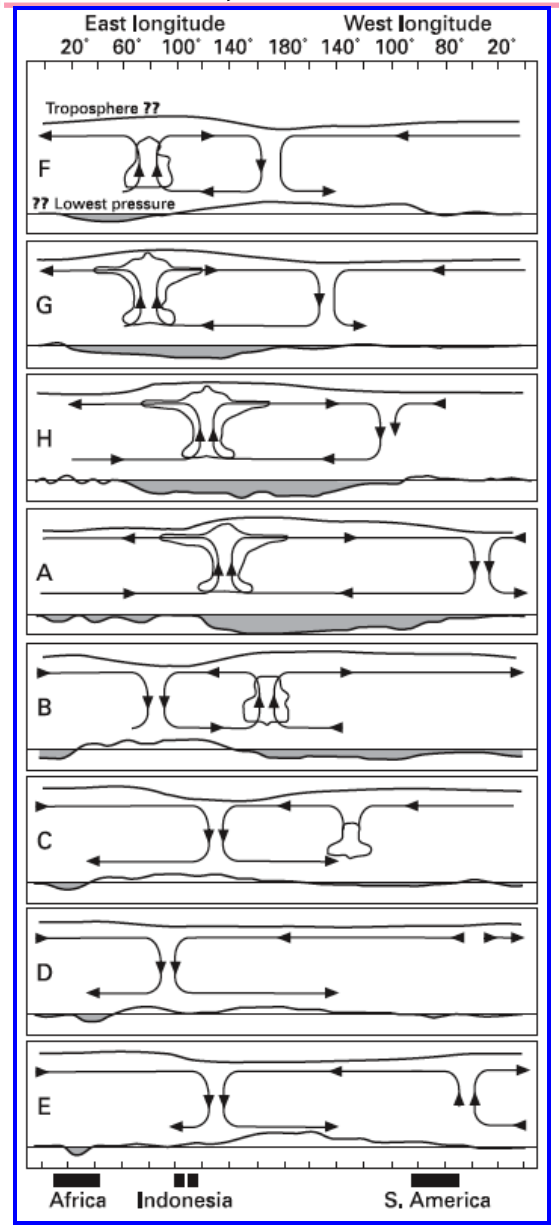

Madden & Julian, 1972

The first documentation of the tropical intraseasonal oscillation based on modern instrumental data was given by Madden and Julian in their pioneering studies (Madden and Julian 1971, 1972) and hence the MJO.

Their observations were based on atmospheric rawinsonde data of about 10 years collected from a broad tropical Indian and Pacific region.

Their observation of the gross structure and evolutionary behavior of the tropical intraseasonal oscillation still serves as the classic, text-book standard description of this phenomenon.

Ref. Chidong Zhang, Waliser et al.

Madden-Julian Oscillation

Subsequent observations up to date using more advanced technology have only added details to theirs.

Observations of the ISO have experienced two major advancements.
One is the use of global data such as satellite data, have allowed us to gain a global view of the phenomenon.
The second is the use of oceanic observations, which have allowed us to appreciate the air-sea interaction nature of the ISO.

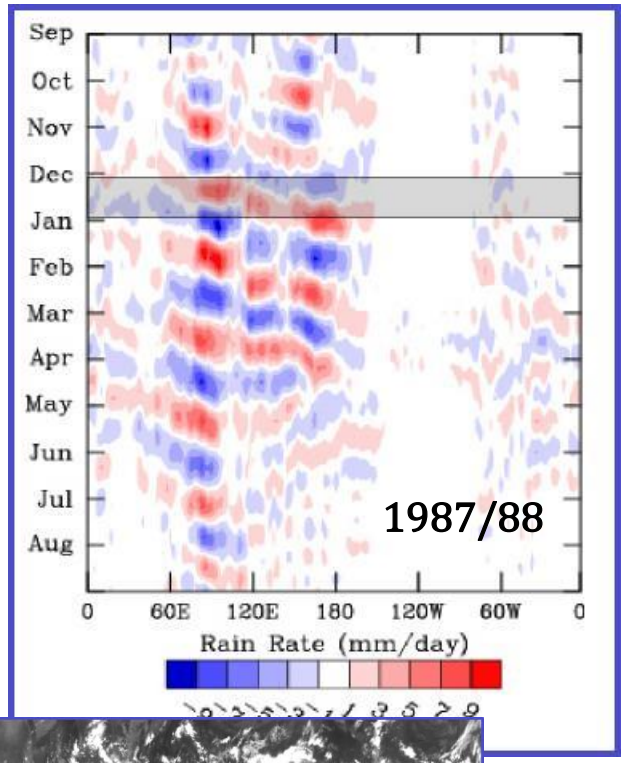

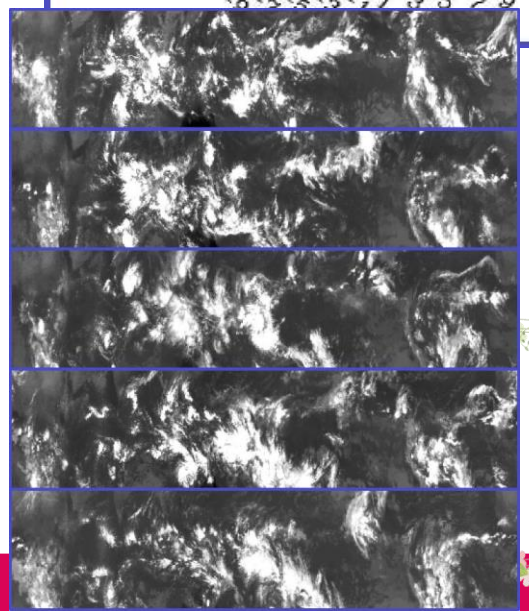

Ref. Waliser et al.

Madden-Julian Oscillation

(a.k.a. Intraseasonal, 40-50, 30-60 Day Oscillation)

- Intraseasonal Time Scale: ~40-60 days
- Planetary-Scale: Zonal Wavenumbers 1-3
- Baroclinic Wind Structure
- Convection Has Multi-Scale Structure
- Eastward Propagation
  - ✓E. Hem: ~5 m/s, Surf.+Conv.+Circ. Interactions
  - ✓W. Hem: ~ > 10 m/s, ~Free Tropospheric Wave
- Tendency to be Equatorially Trapped
- Strong Seasonal Dependence:
  - ✓ NH Winter: Eastward Propagation
  - ✓ NH Summer: ~Northeast Propagation
- Significant Interannual Variability
- Significant Remote and Extra-Tropical Impacts

MJO

Ref. Waliser et al.

OLR Spectra
Winter vs.
Summer

In summer the power is more Concentrated, and it occurs at a higher frequency than during winter

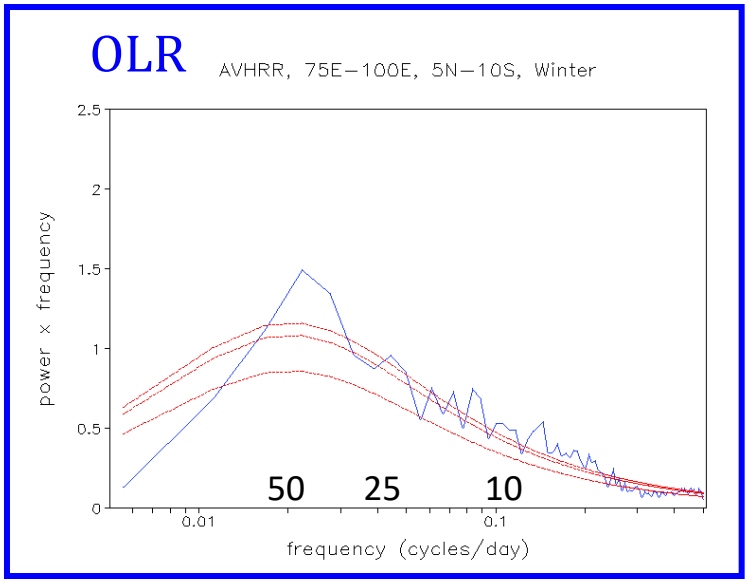

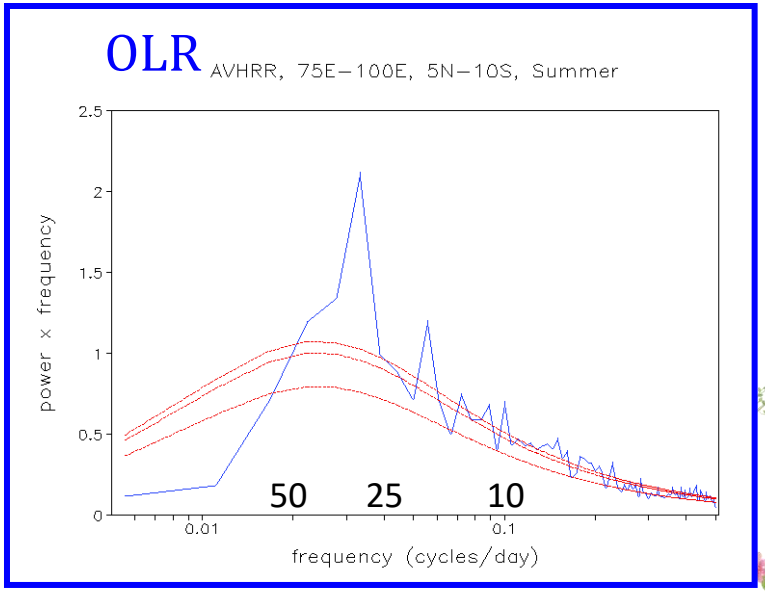

MJO

Wavenumber Frequency Diagrams

Roughly Wavenumbers 1-3 Periods 30-70 Days

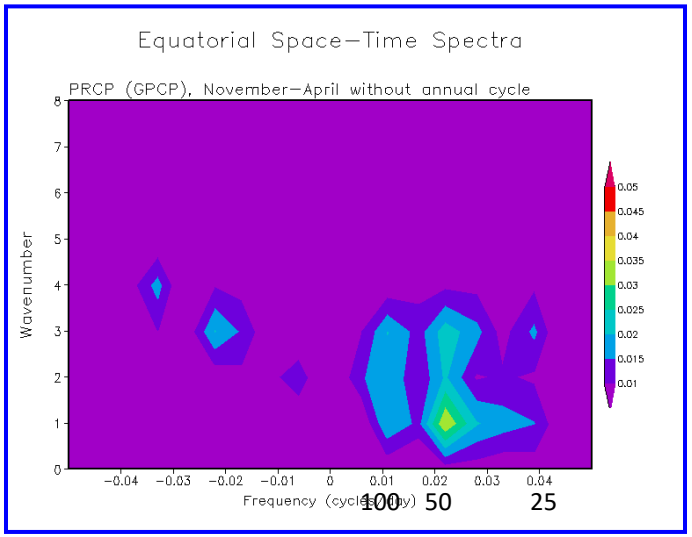

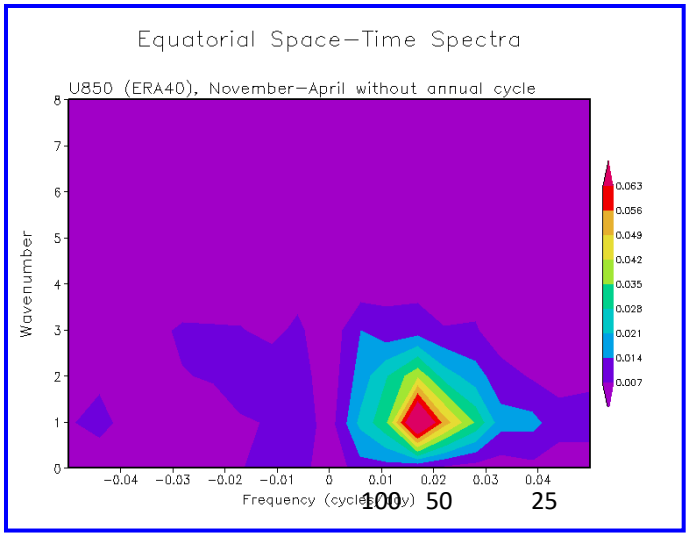

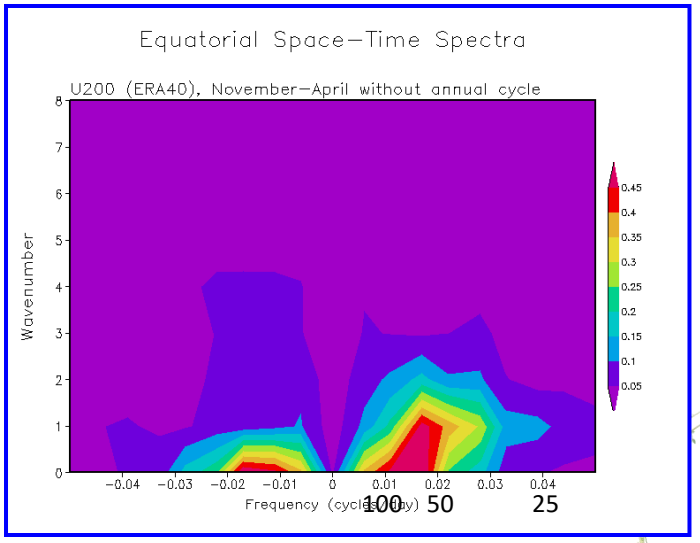

MJO

Madden-Julian Oscillation

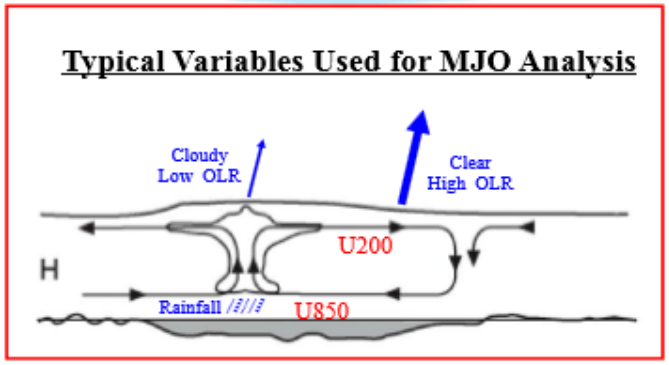

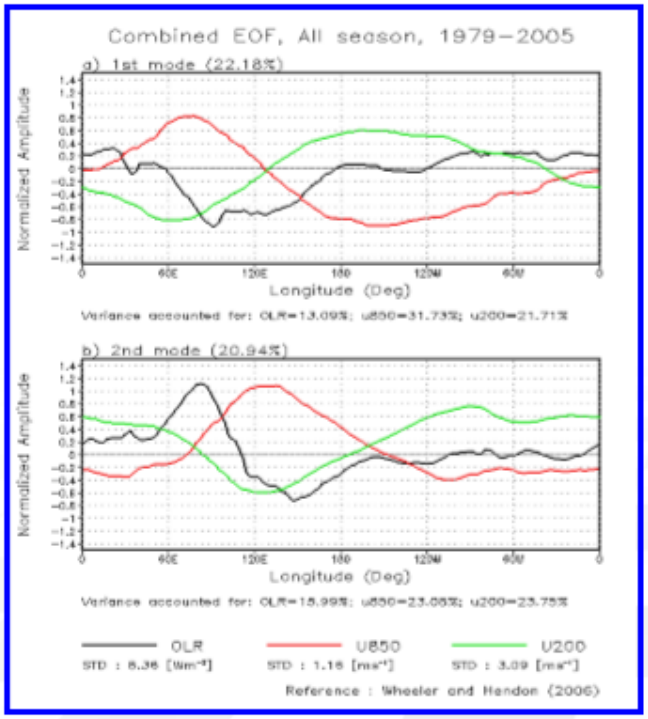

Wheeler an Hendon (2004)

- As a measure of the strength of the MJO, **Realtime Multivariate MJO (RMM) index** is defined using the **first two leading multivariate EOF modes of the equatorial mean (between 15S and 15N) OLR, and zonal winds at 850 and 200 hPa (Wheeler and Hendon, 2004)**.

- The **RMM index** captures equatorial eastward propagating mode, the MJO, very well and has been applied all year around to depict MJO activity.

Ref. Waliser et al.

Madden-Julian Oscillation

Convectively Coupled Equatorial Waves

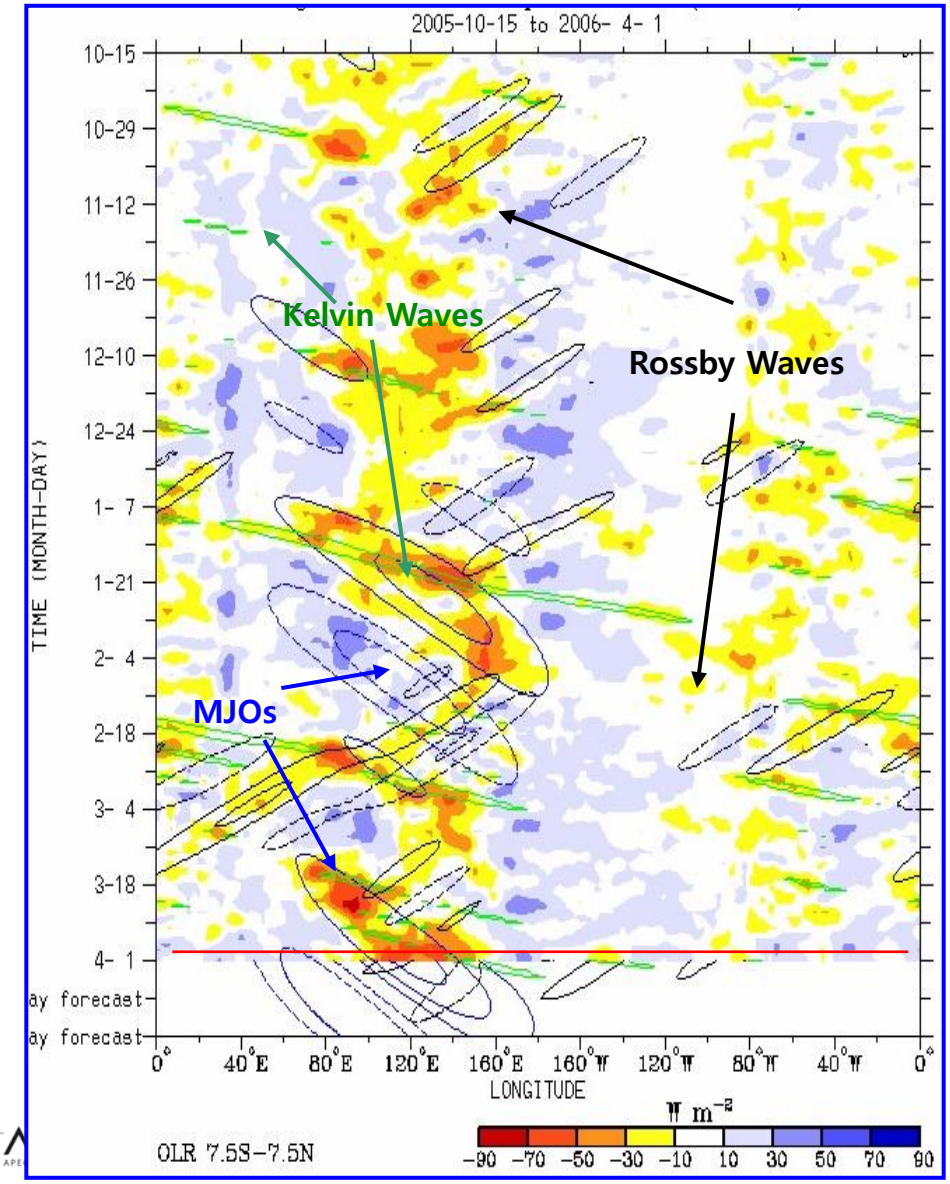

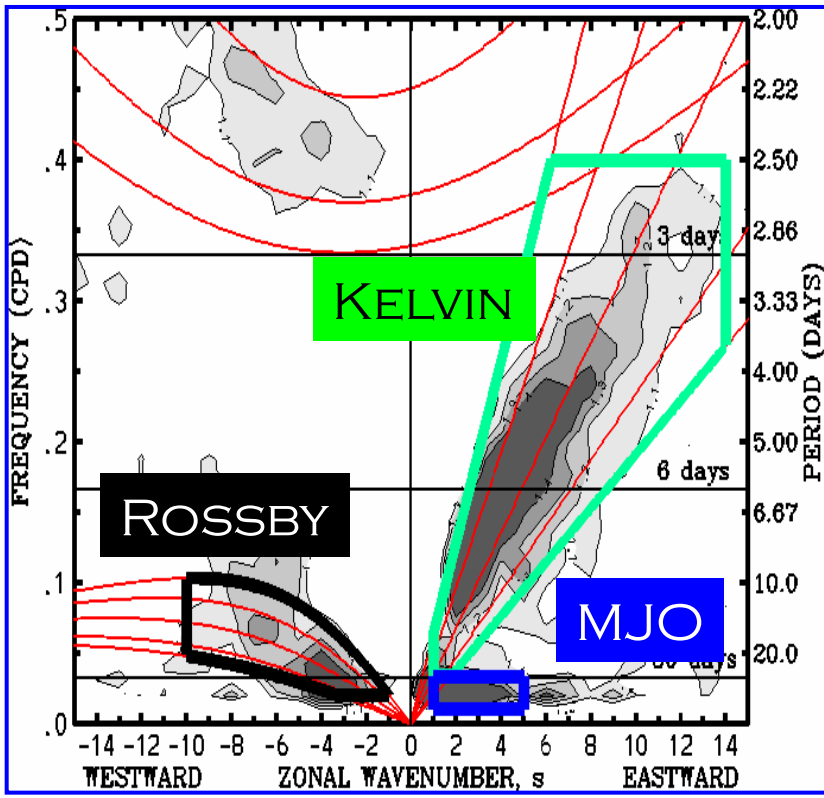

MJO

Ref. Wheeler

2 Seaseonal dependence of ISO

How ISO behavior is affected by annual cycle?

boreal winter (MJO)

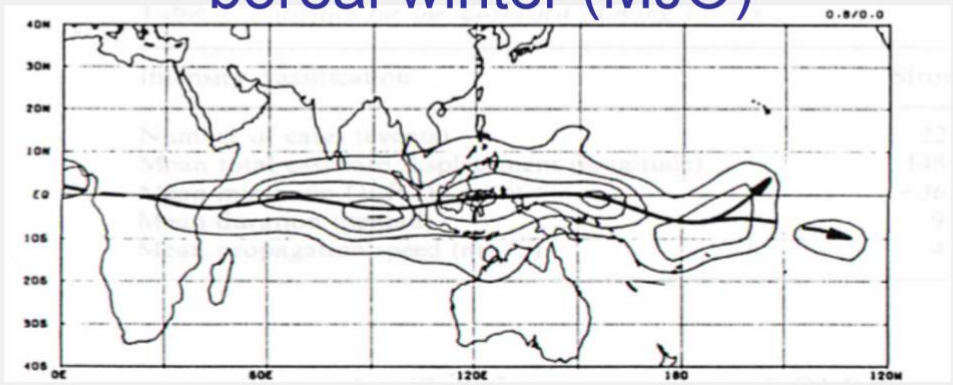

boreal summer (BSISO)

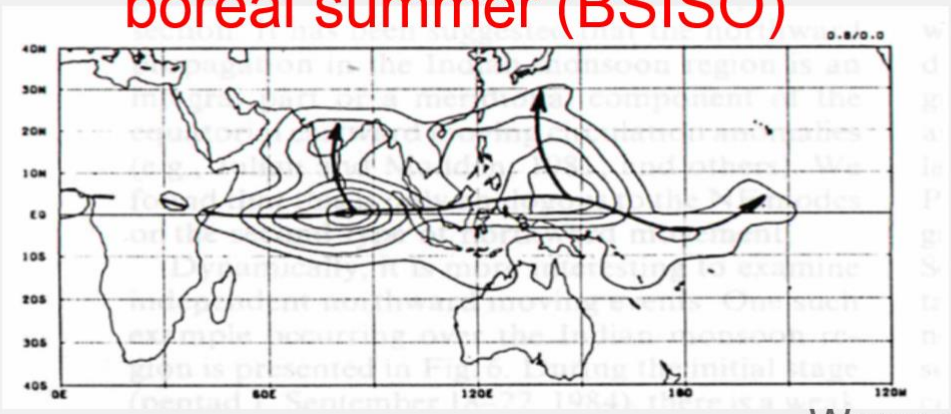

Wang and Rui 1990

Seasonal dependence

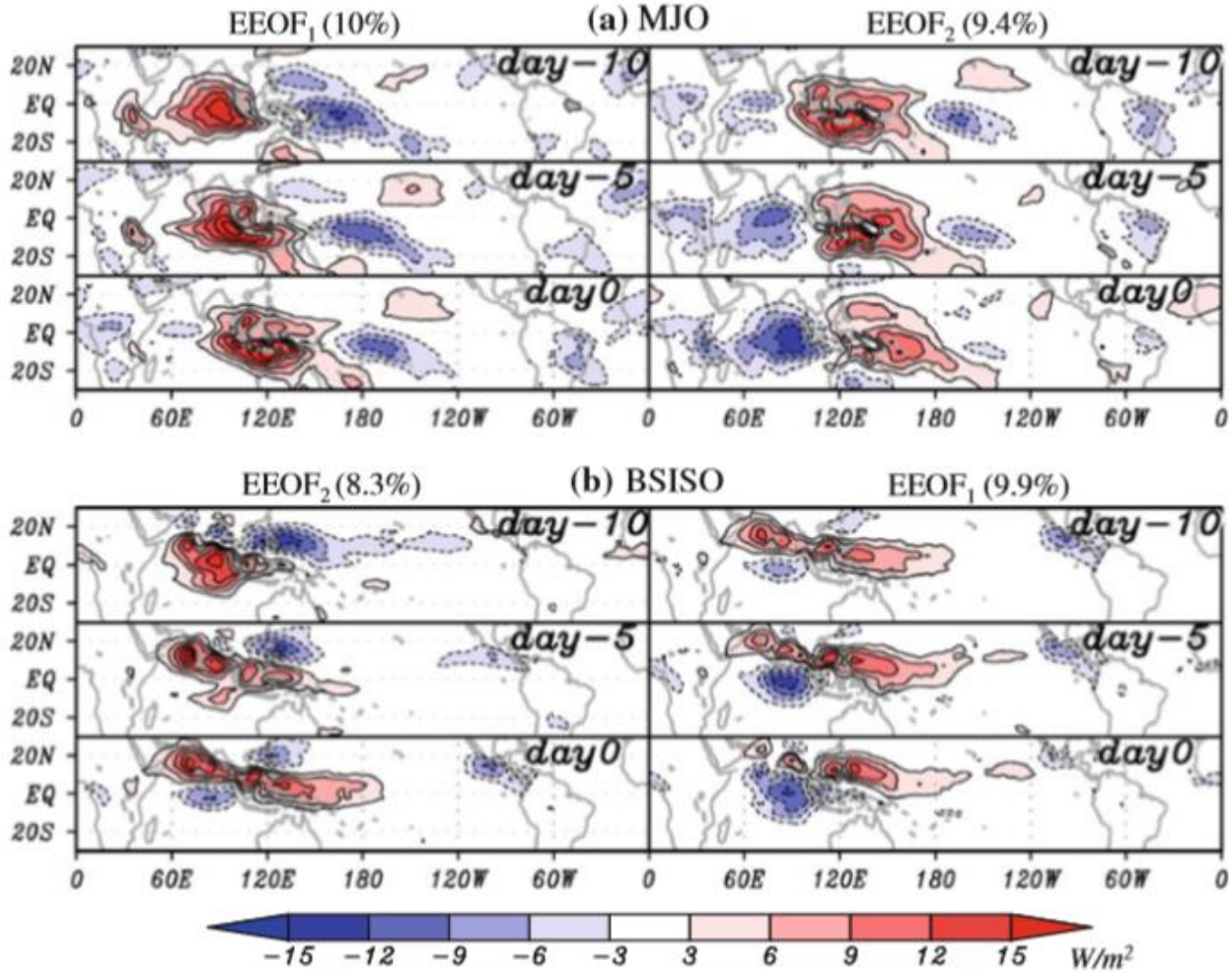

Fig. 2 Spatial-temporal pattern of OLR anomaly associated with the intraseasonal oscillation during (**a**) boreal winter (DJF, referred to as MJO mode) and (**b**) boreal summer (JJA, referred to as BSISO mode) by means of the extended EOF (EEOF) analysis.

Ref. Kikuchi et al.

Seasonal dependence

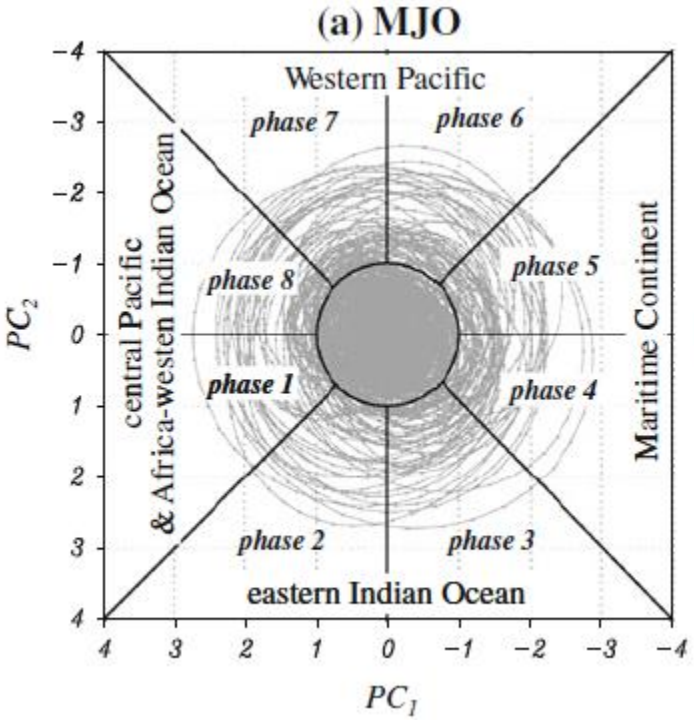

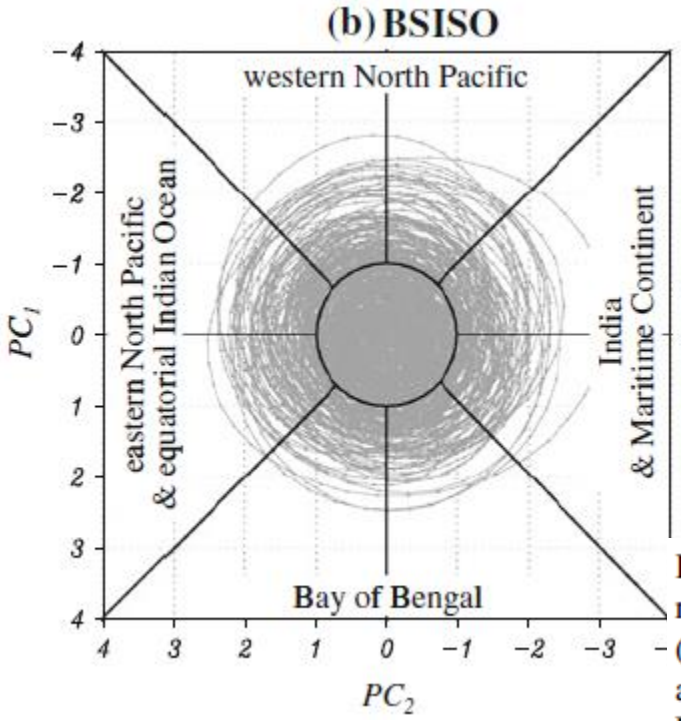

Fig. 7 Phase space representation of the state of (**a**) the MJO mode (PC_2, PC_1) and (**b**) the BSISO mode (PC_1, PC_2) for the period 1979–2009. The state of the ISO categorized as eight phases are used for the following discussion. The approximate positions of the major convective area at some phases are also denoted. Note that each PC is normalized by one standard deviation of the corresponding PCs during the period each EEOF analysis was performed to obtain the EEOFs

Ref. Kikuchi et al.

Seasonal dependence

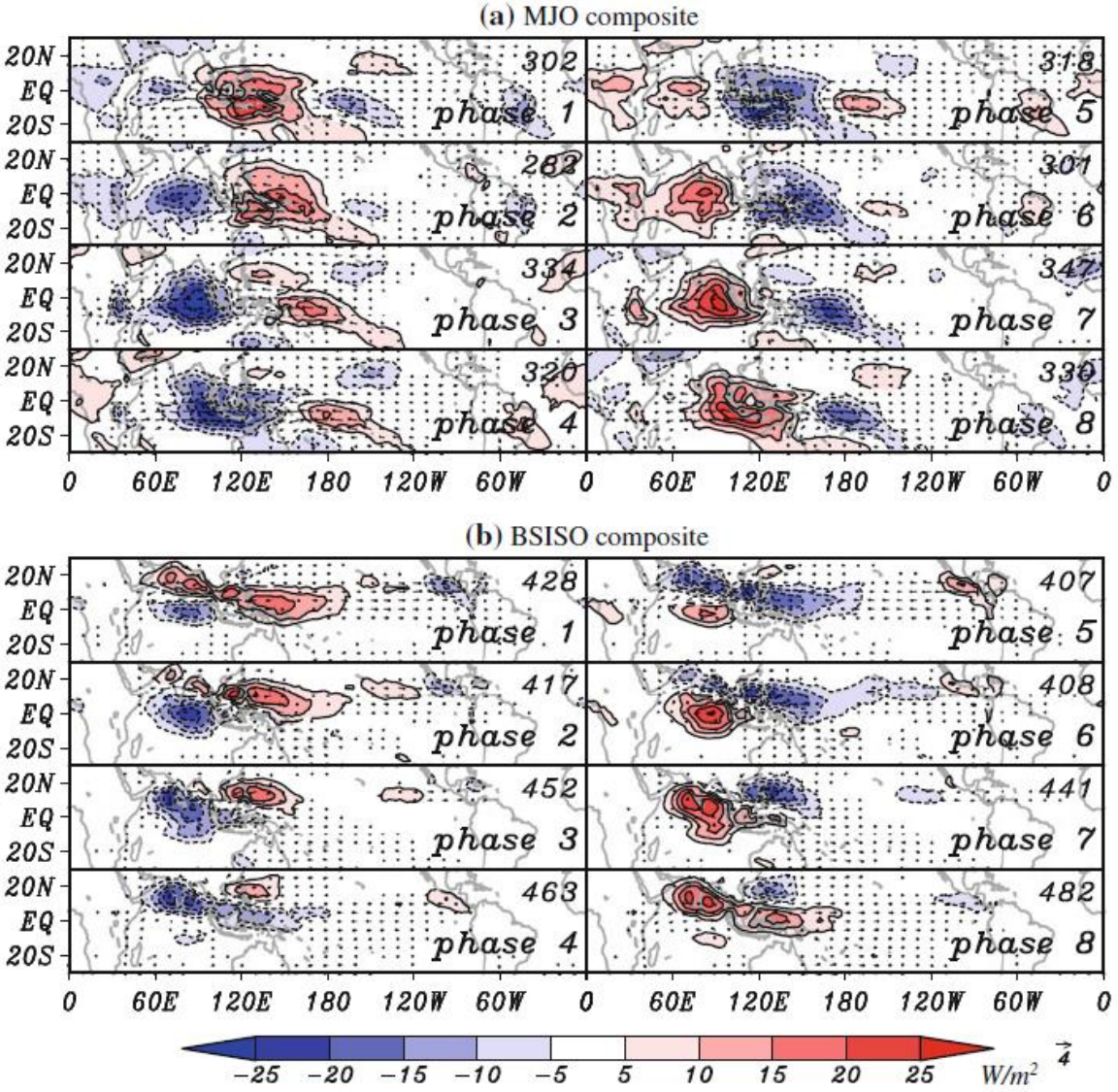

Fig. 8 Composite life cycle of (**a**) the MJO mode and (**b**) the BSISO mode. OLR anomalies (shades and contours of 5 Wm^{-2}) and 850 hPa horizontal winds (*vectors*). Significant values at the 99% level according to the *t* test with degree of freedom being one sixth of the number of composite samples (taking into account of persistence) are only drawn. The number of composite samples are denoted in the *upper right* corner of each *panel*

Ref. Kikuchi et al.

Seasonal dependence

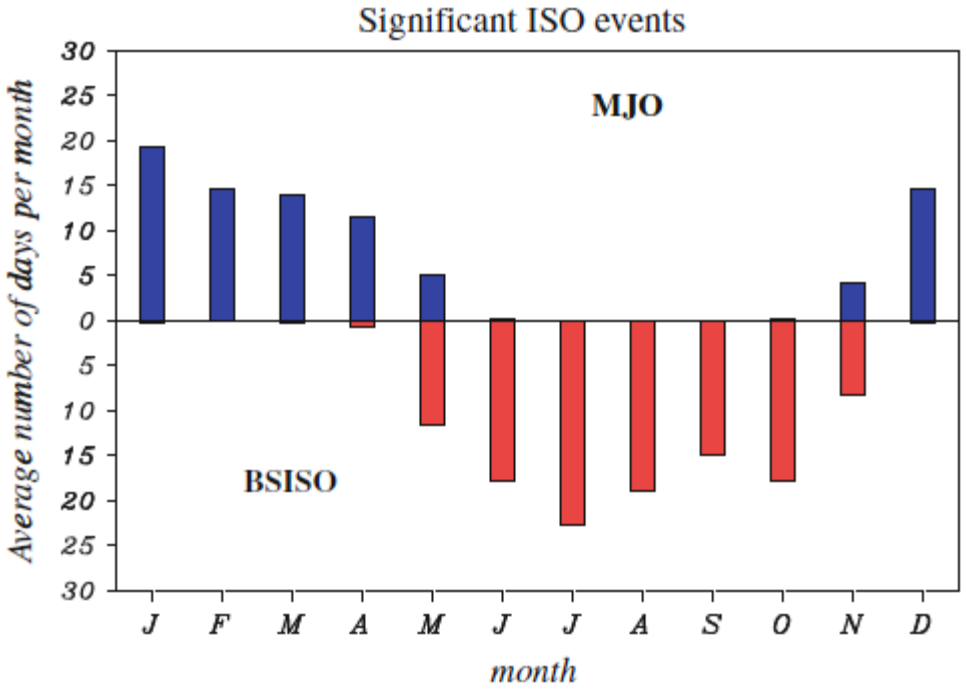

Fig. 9 Average number of days during which significant ISO is present in a month. The days are normalized such that they are the ratio of the number of days classified as the significant MJO mode (*upper*) or significant BSISO mode (*lower*) to the available number of days during 1979–2009 times the number of days in the month of common year

Ref. Kikuchi et al.

3 Interannual variability

Interannual variability

In the Pacific, interannual variability in zonal wind variance of the MJO is more prominent in the lower than upper troposphere [*Gutzler*, 1991]. During a warm event of ENSO , as the eastern edge of the warm pool extends eastward [*Picaut et al.*, 1996], so does MJO activity

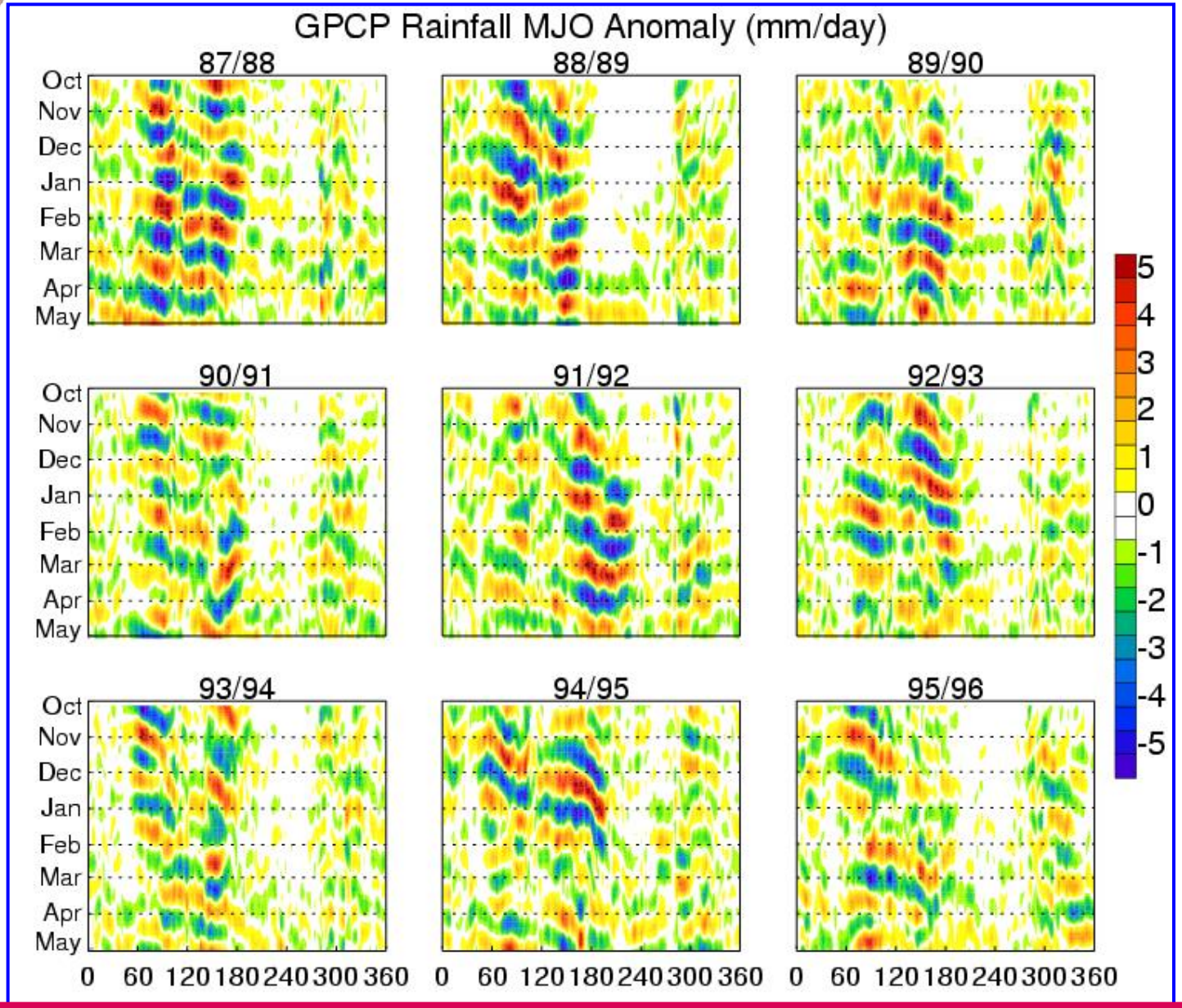

APCC APEC CLIMATE CENTER

Ref. Waliser et al.

Predominant low-frequency modes in the tropical atmosphere

ENSO

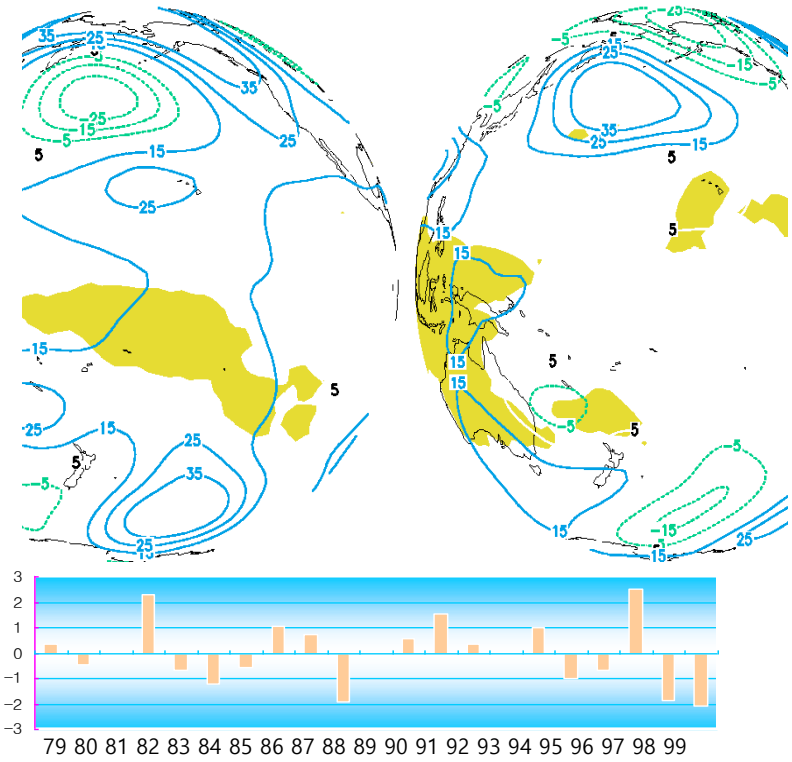

MJO

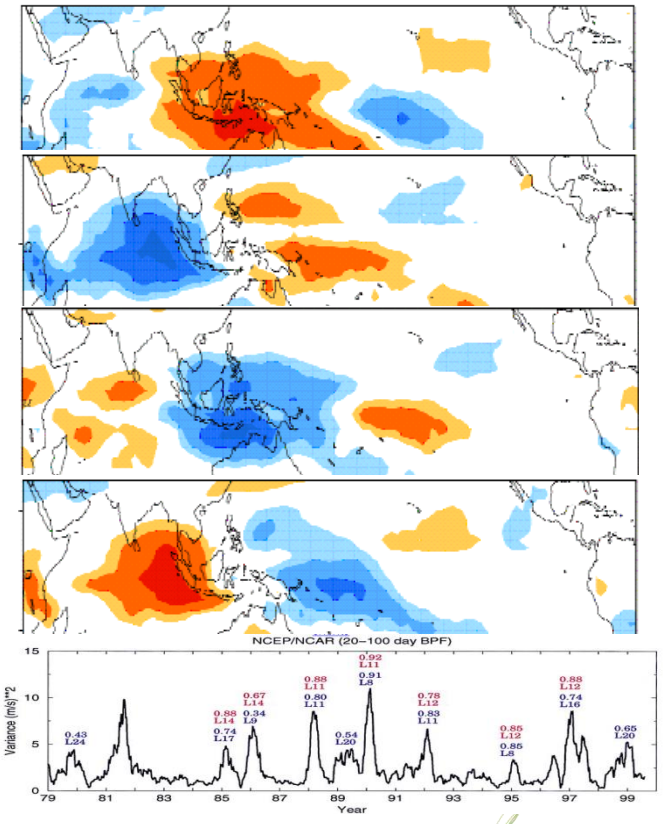

Intraseasonal Variance during ENSO

El Nino

(a) OLR

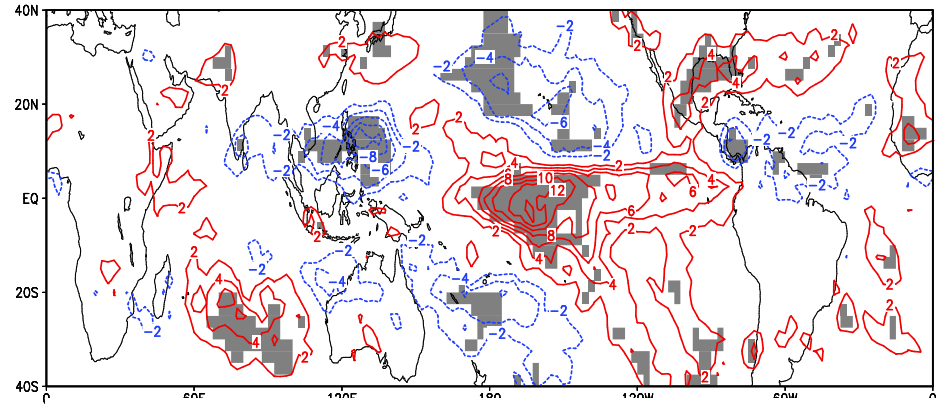

(b) Streamfunction(850hPa)

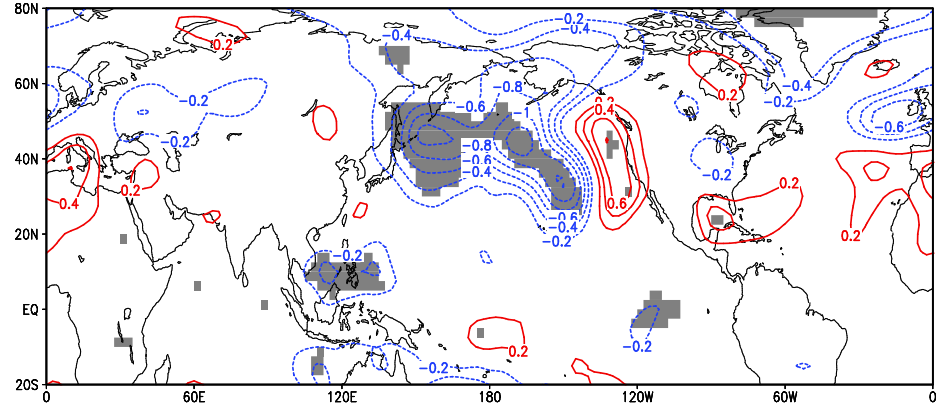

La Nina

(a) OLR

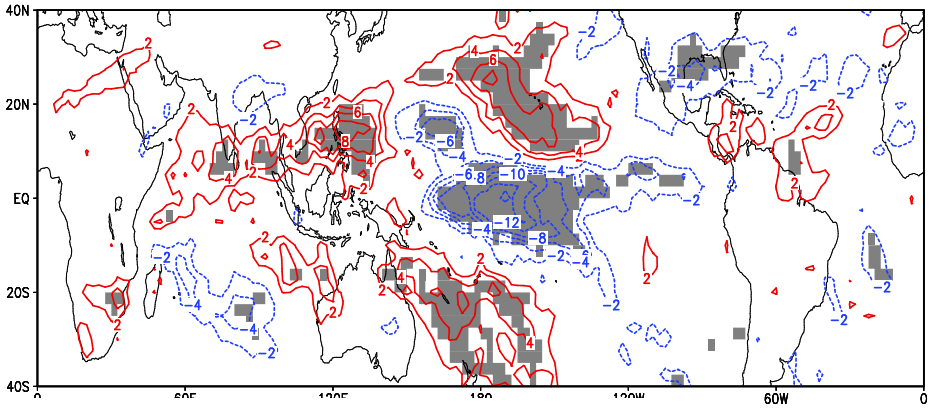

(b) Streamfunction(850hPa)

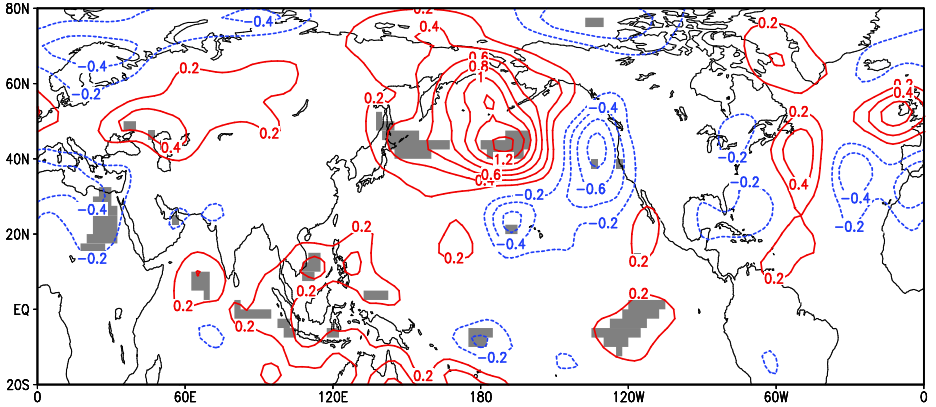

ENSO regulation of MJO teleconnection

El Nino

La Nina

(a) Phase 3 (300hPa)

(b) Phase 3 (300hPa)

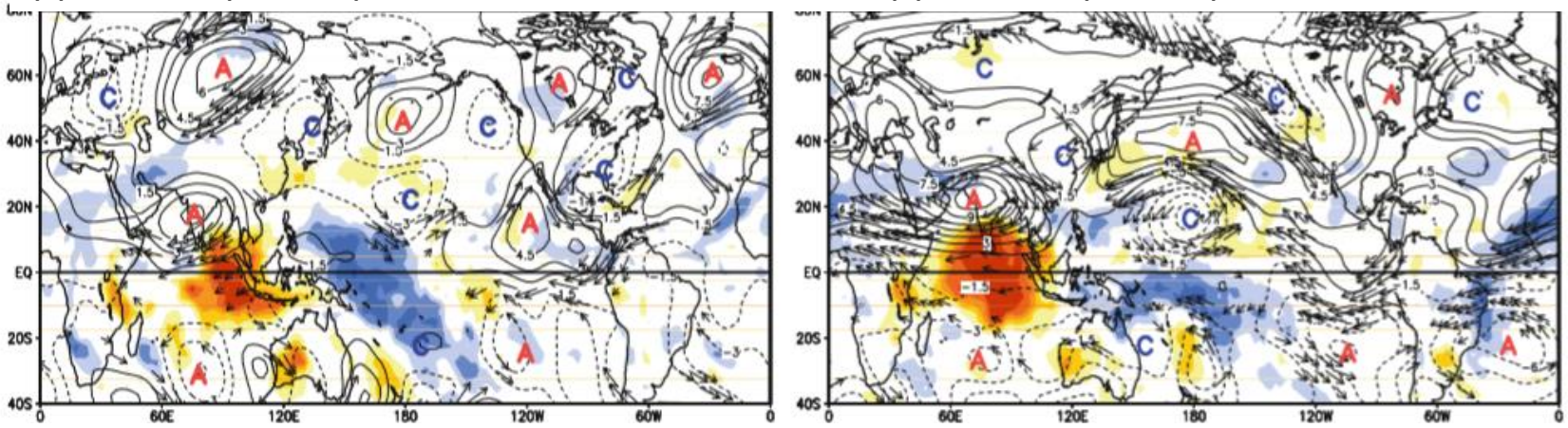

(c) Phase 3 (850hPa)

(d) Phase 3 (850hPa)

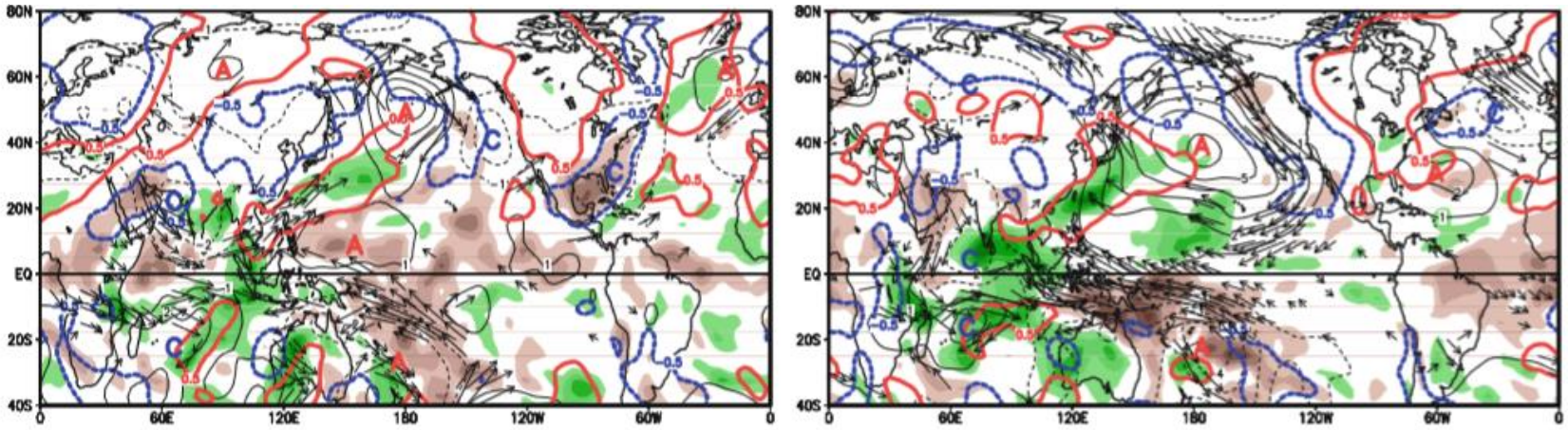

For OLR

For Precipitable water

Fig: Composite anomalies of (a)(b) SF300 (contours) and winds and (c)(d) SF850 (contours)and winds during El Niño (left panel) and La Niña years (right panel) at Phase3 (when the convection is enhanced over Indian ocean). OLR and precipitable water during ENSO are shaded in (a)~(b) and (c)~(d), respectively. In (c) and (d) and the red (blue) thick contours denote the 850 hPa temperature anomalies above (below) 0.5 (-0.5) ºC.

ENSO regulation of MJO teleconnection

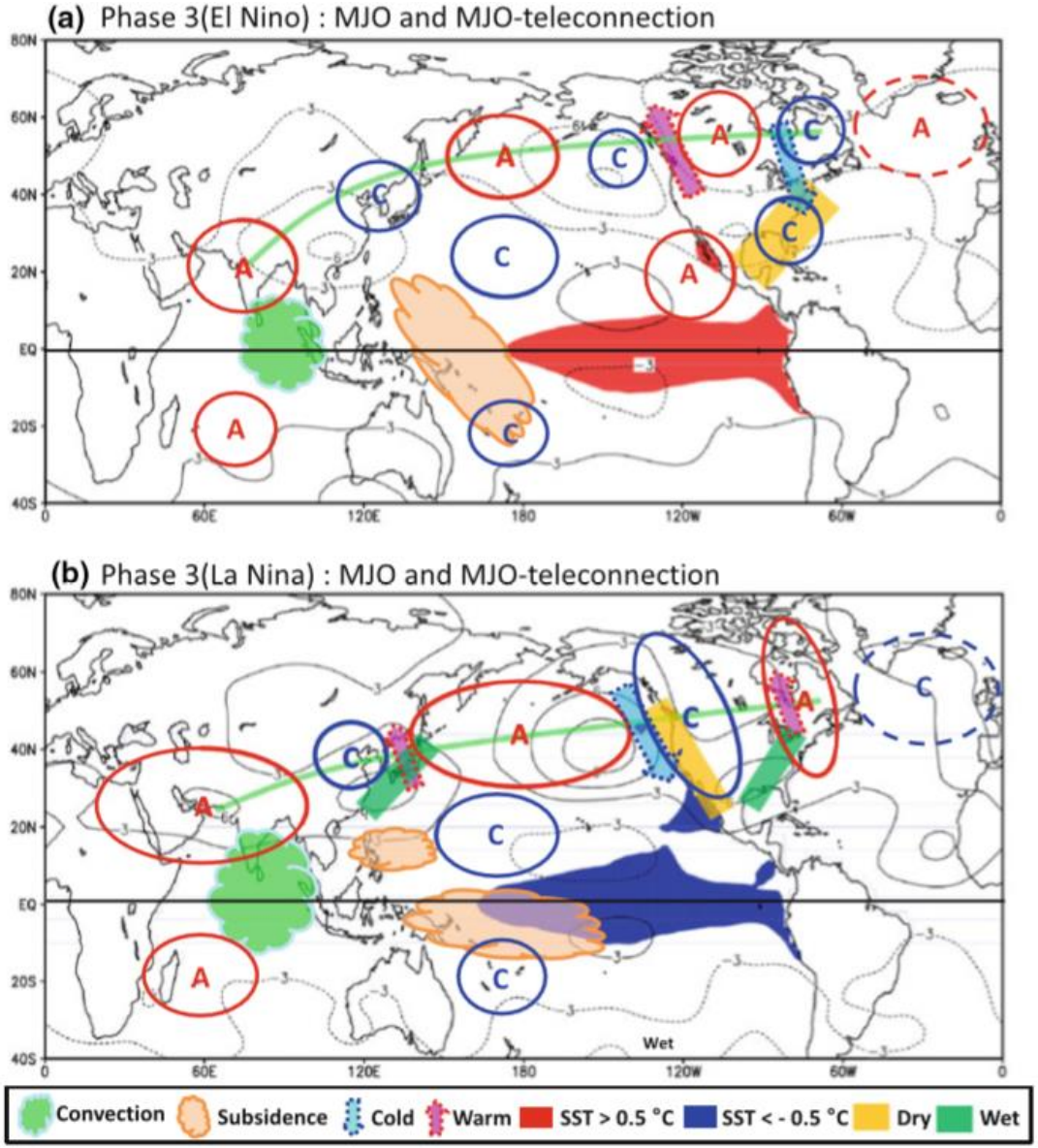

ENSO regulation of MJO teleconnection

El Nino

La Nina

(a) Phase 7 (300hPa)

(b) Phase 7 (300hPa)

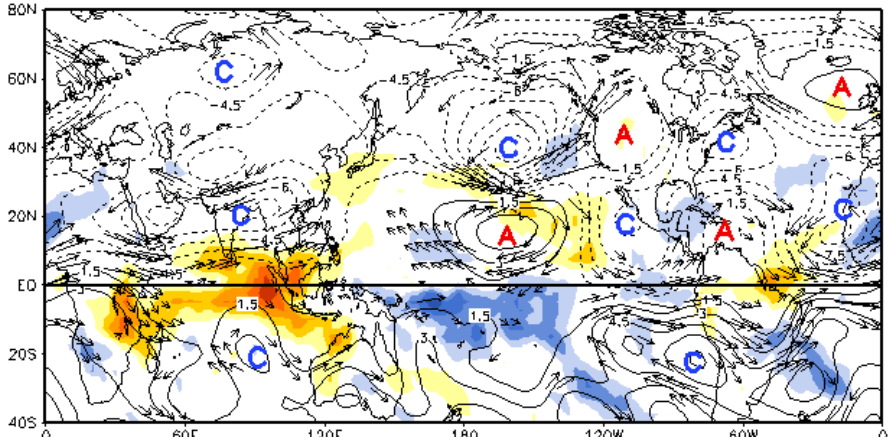

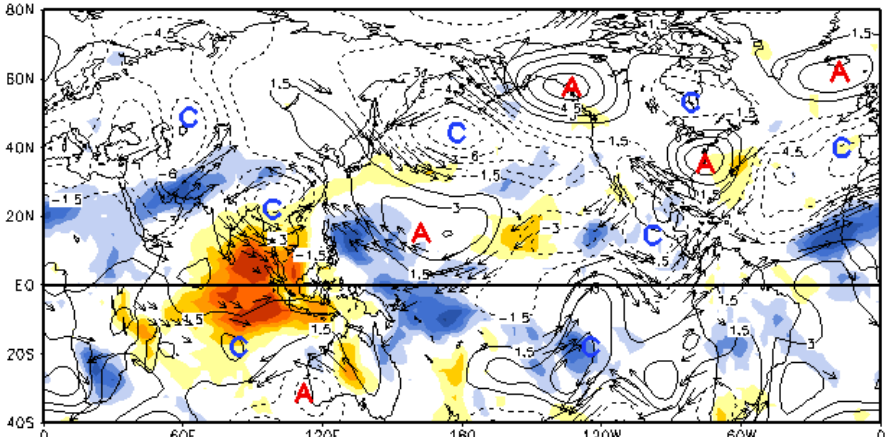

(c) Phase 7 (850hPa)

(d) Phase 7 (850hPa)

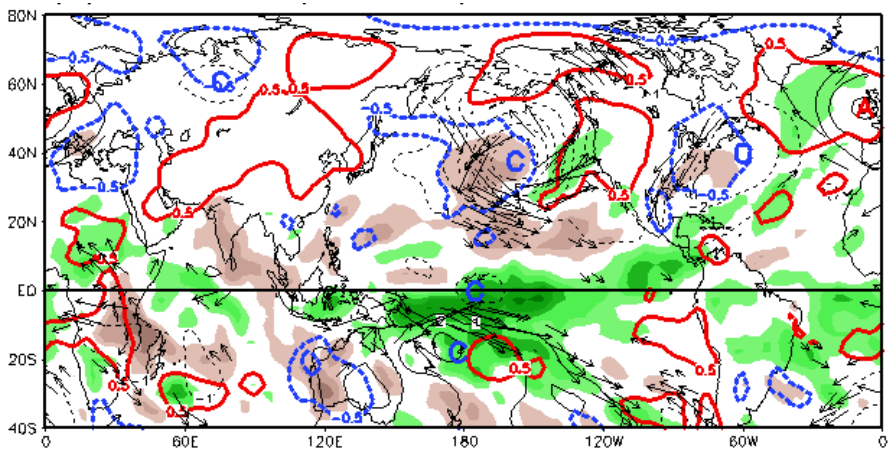

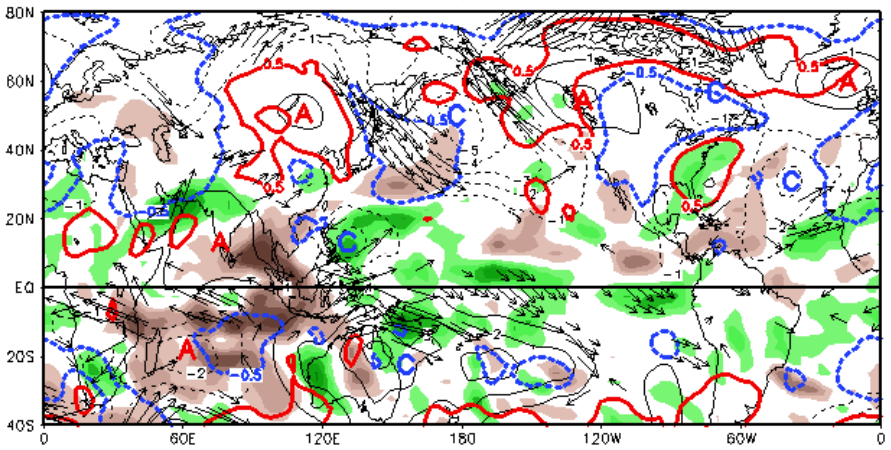

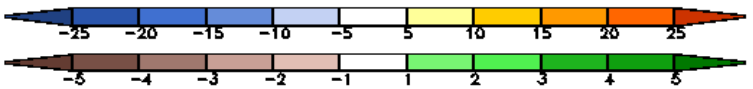

For OLR

For Precipitable water

Fig: Composite anomalies of (a)(b) SF300 (contours) and winds and (c)(d) SF850 (contours)and winds during El Niño (left panel) and La Niña years (right panel) at Phase 7 (when the convection is enhanced over western Pacific). OLR and precipitable water during ENSO are shaded in (a)~(b) and (c)~(d), respectively. In (c) and (d) and the red (blue) thick contours denote the 850 hPa temperature anomalies above (below) 0.5 (-0.5) ºC.

ENSO regulation of MJO teleconnection

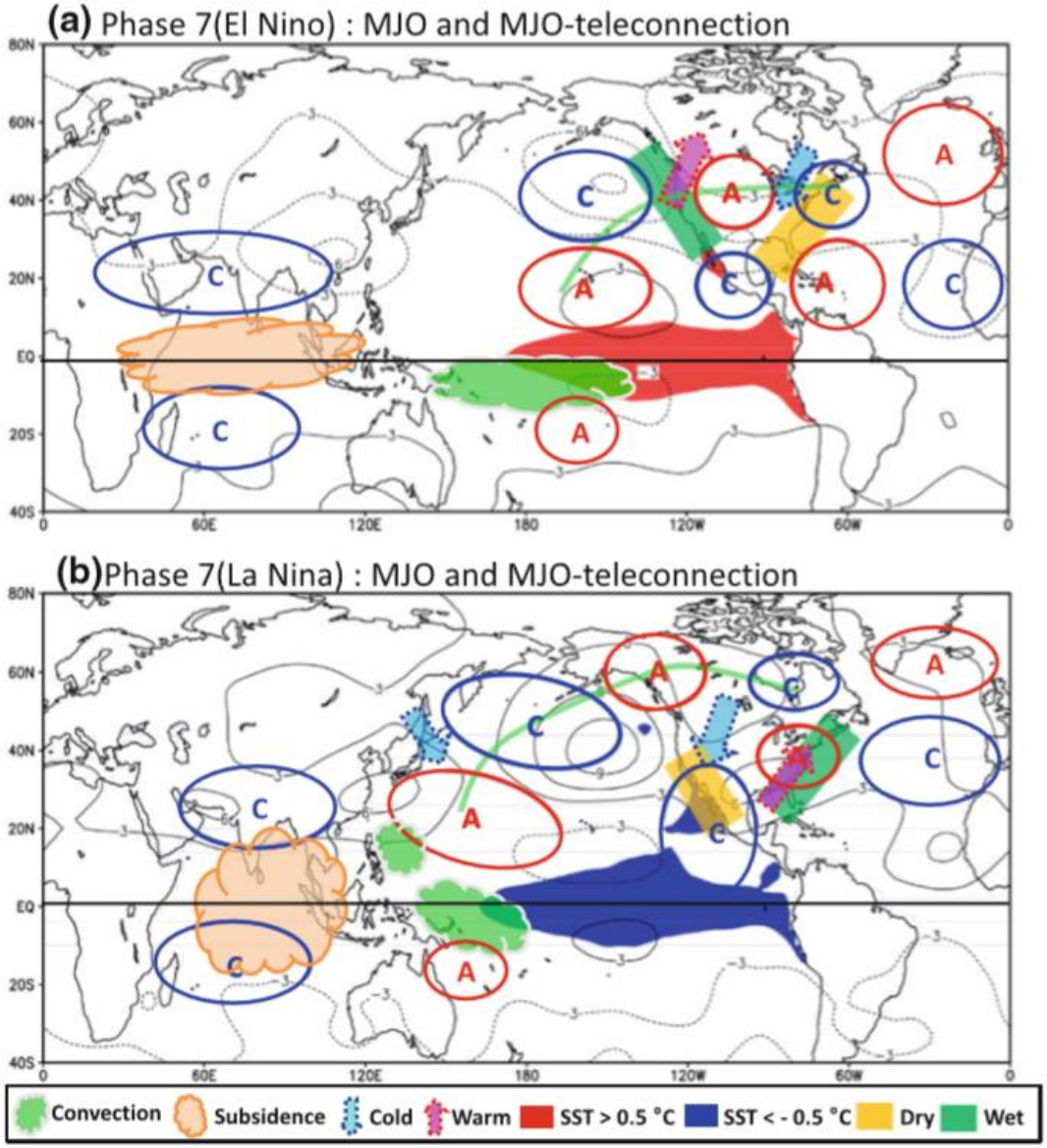

Longer-Term Variability of MJO/ISO

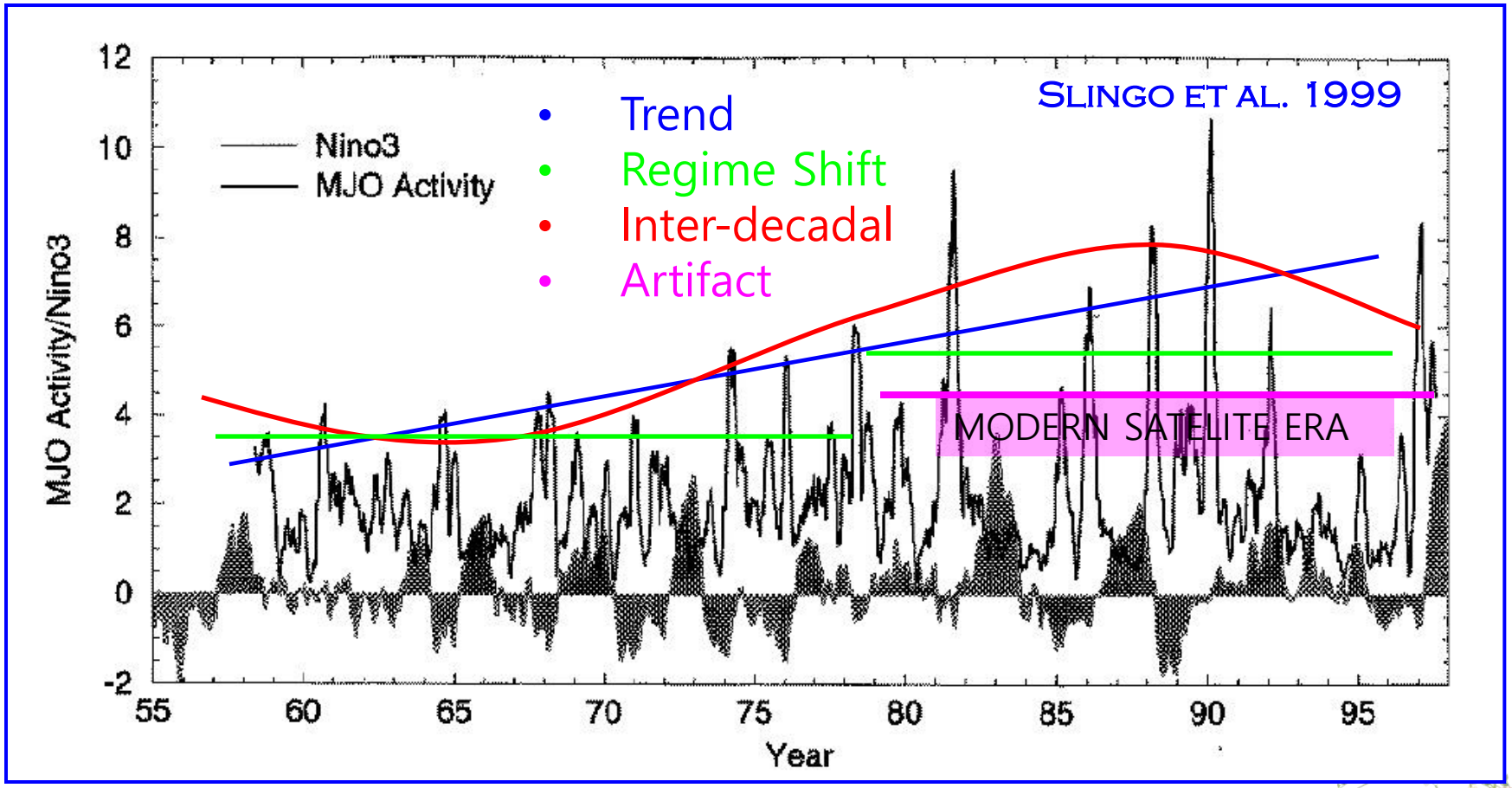

Ref. Waliser et al.

4 Teleconnection

- Weather and Climate Impacts

APCC
APEC CLIMATE CENTER

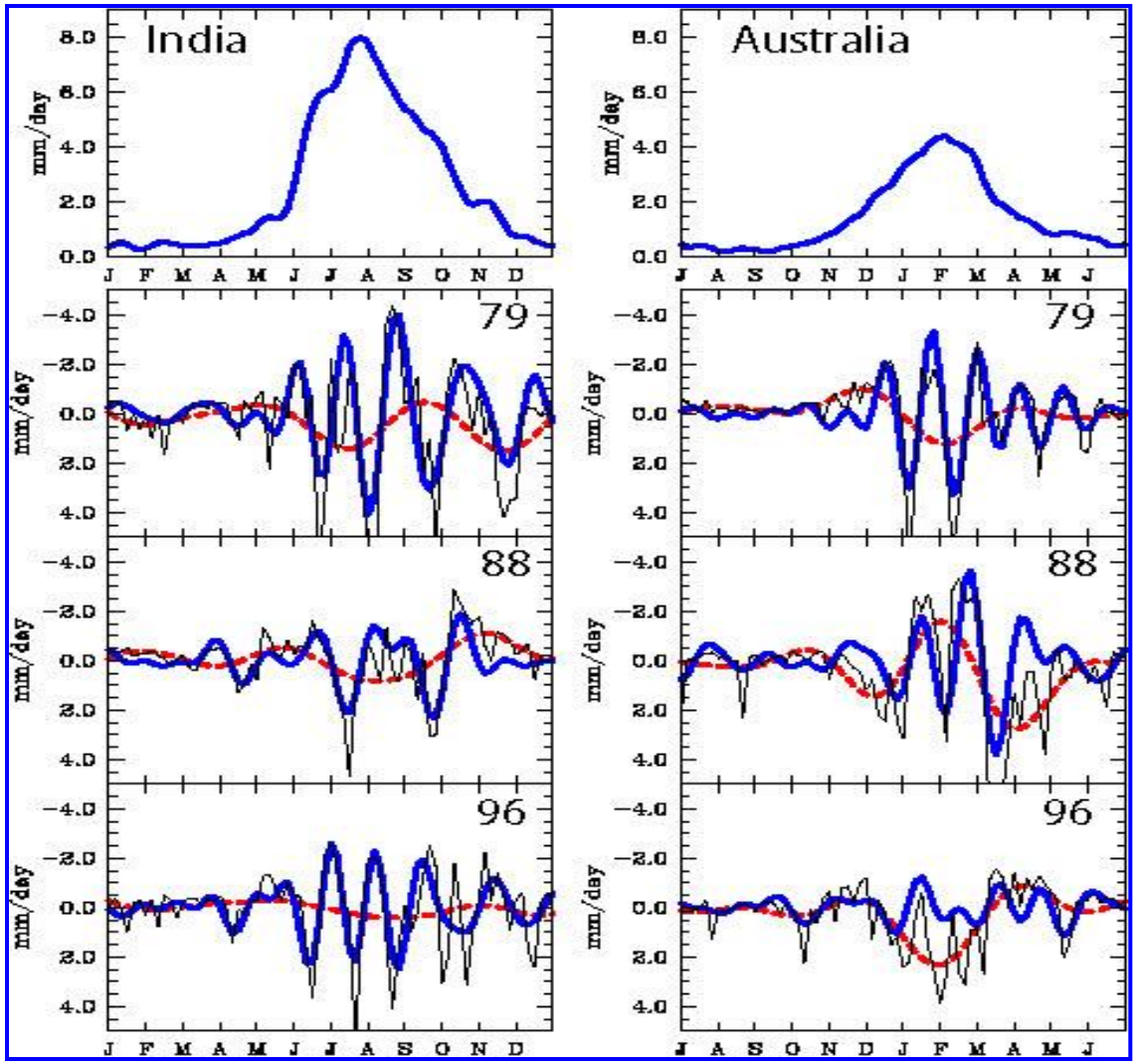

Onsets & Breaks of The Asian & Australian Summer Monsoon

Ref. Waliser et al.

Indian Monsoon Onset & Heavy Rainfall

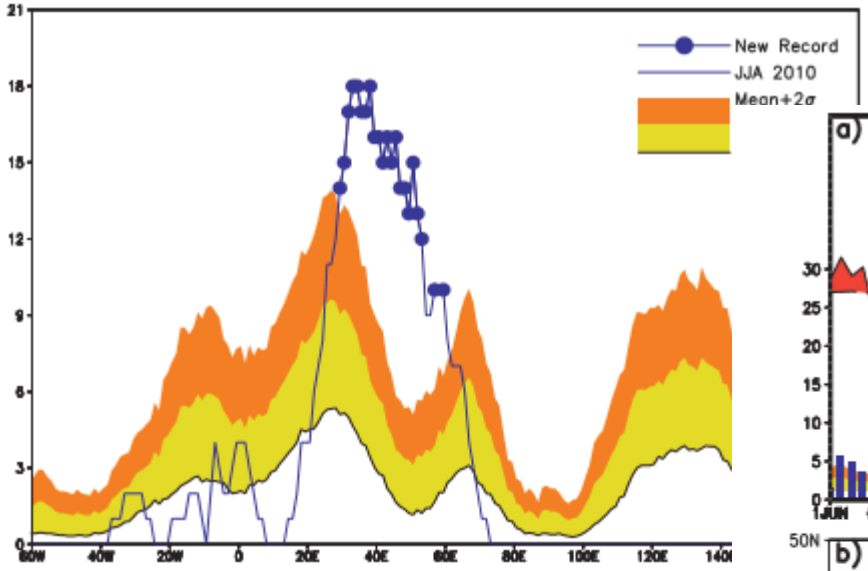

FIG. 2. Number of blocking events at each longitude during boreal summer (blue) and climatological mean distribution of atmospheric blocking from 1979 and orange layers indicate 1 and 2 std dev from mean, respectively. Blue dots tudinal locations where the blocks in 2010 were at an all-time high since 1979.

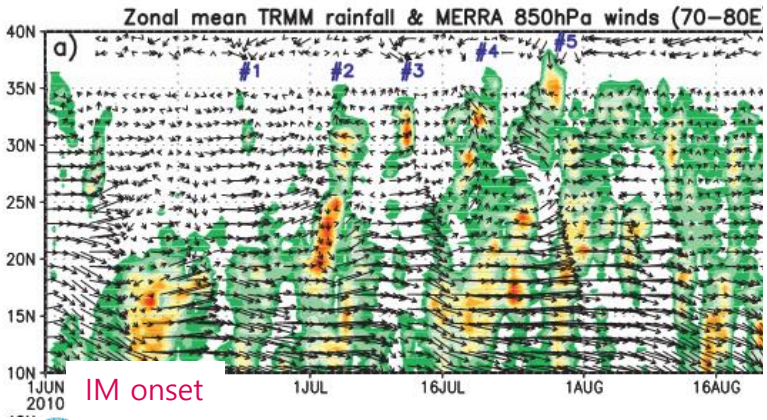

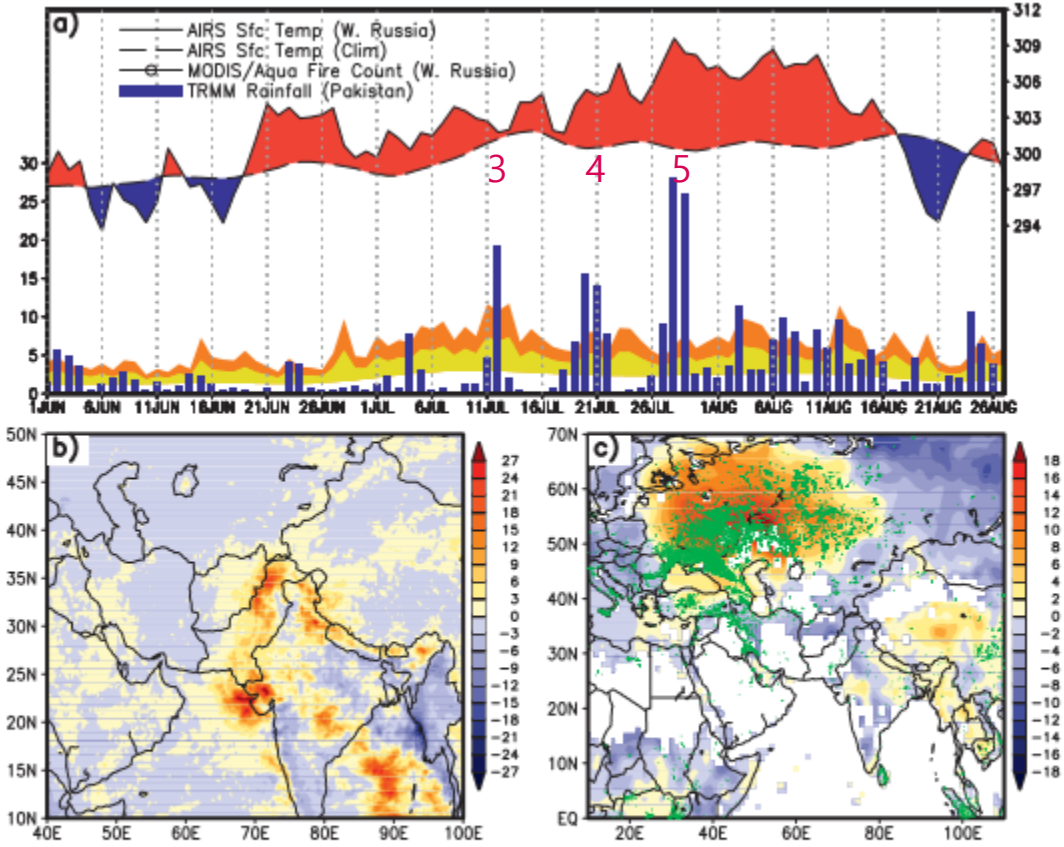

FIG. 1. (a) Time series of AIRS daily surface temperature (°C) averaged over western Russia (45–65°N, 30–60°E), with positive (negative) deviations from climatology shaded red (blue) and TRMM daily rainfall (mm day^{-1}, left ordinate) over northern Pakistan (32–35°N, 70–73°E) for 1 Jun–27 Aug 2010. Spatial distribution of (b) TRMM rainfall anomaly over Pakistan and the South Asian monsoon region for the period 25 Jul–8 Aug 2010, (c) AIRS surface temperature anomaly, and MODIS daily fire pixel (green dots) for the same period. The rainfall anomaly (mm day^{-1}) was derived from the base period of 1988–2009, and the surface temperature anomaly (°C) from the base period of 2003–09.

APCC APEC CLIMATE CENTER

Ref. Lau and Kim

NH SUMMER MONSOON ISO

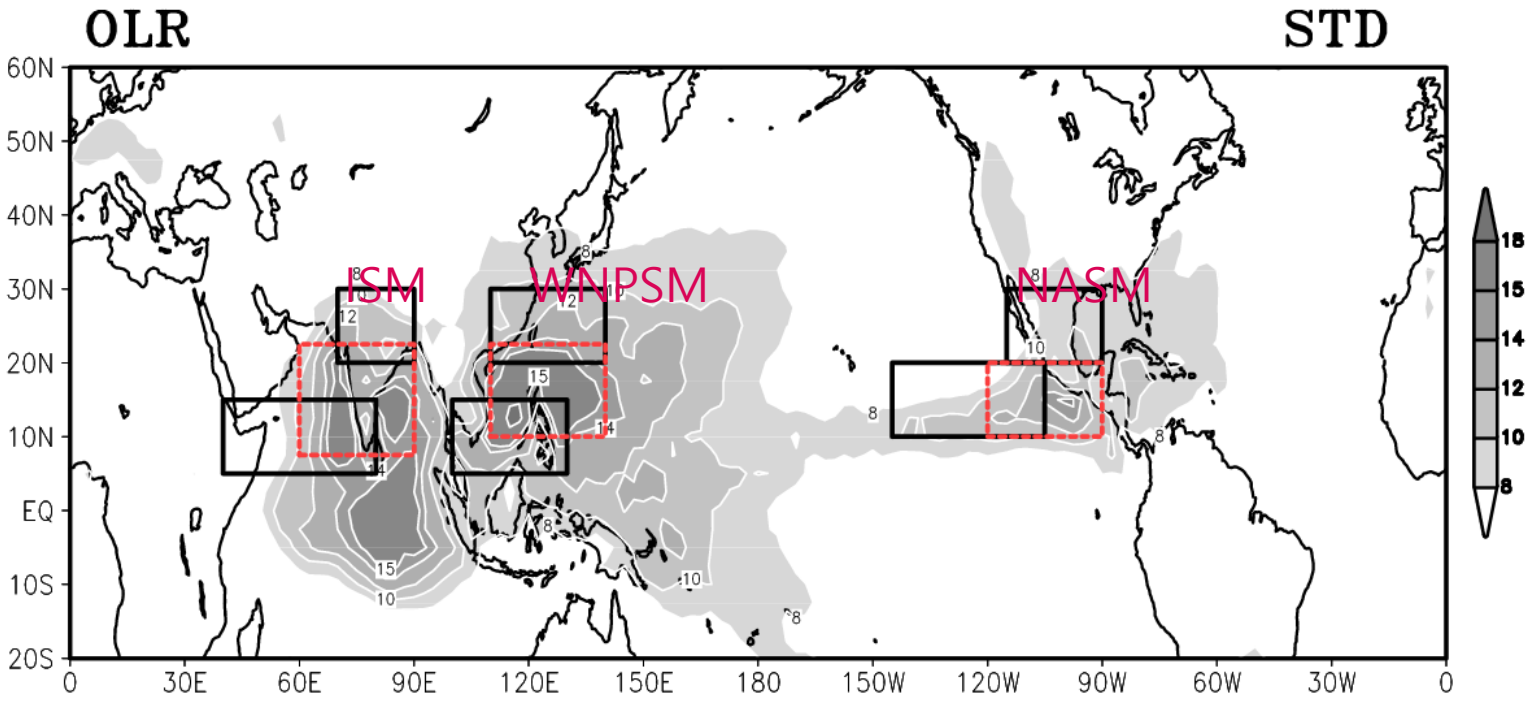

In the NH summer, there are three large convective intraseasonal variability centers along the 10-20ºN latitude bands over the Indian summer monsoon, Western North Pacific summer monsoon, and North American summer monsoon domains

Ref. Moon et al.

Teleconnection

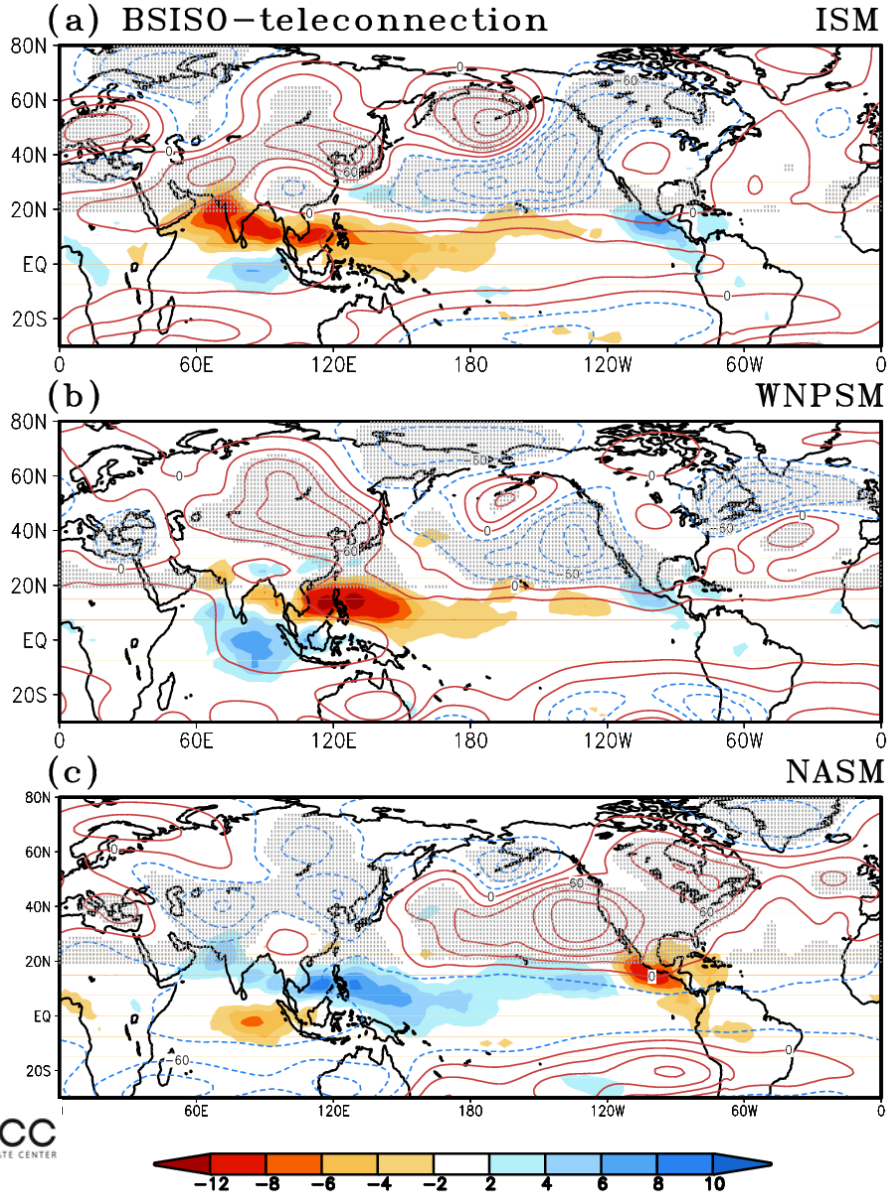

BSISO teleconnections associated with three monsoon ISO centers show

preferred teleconnection centers over the NH continents: Europe, Russia, central Asia, East Asia, western US, and eastern US & Canada, embedded in the waveguide along the jet stream.

Ref. Moon et al.

Teleconnection

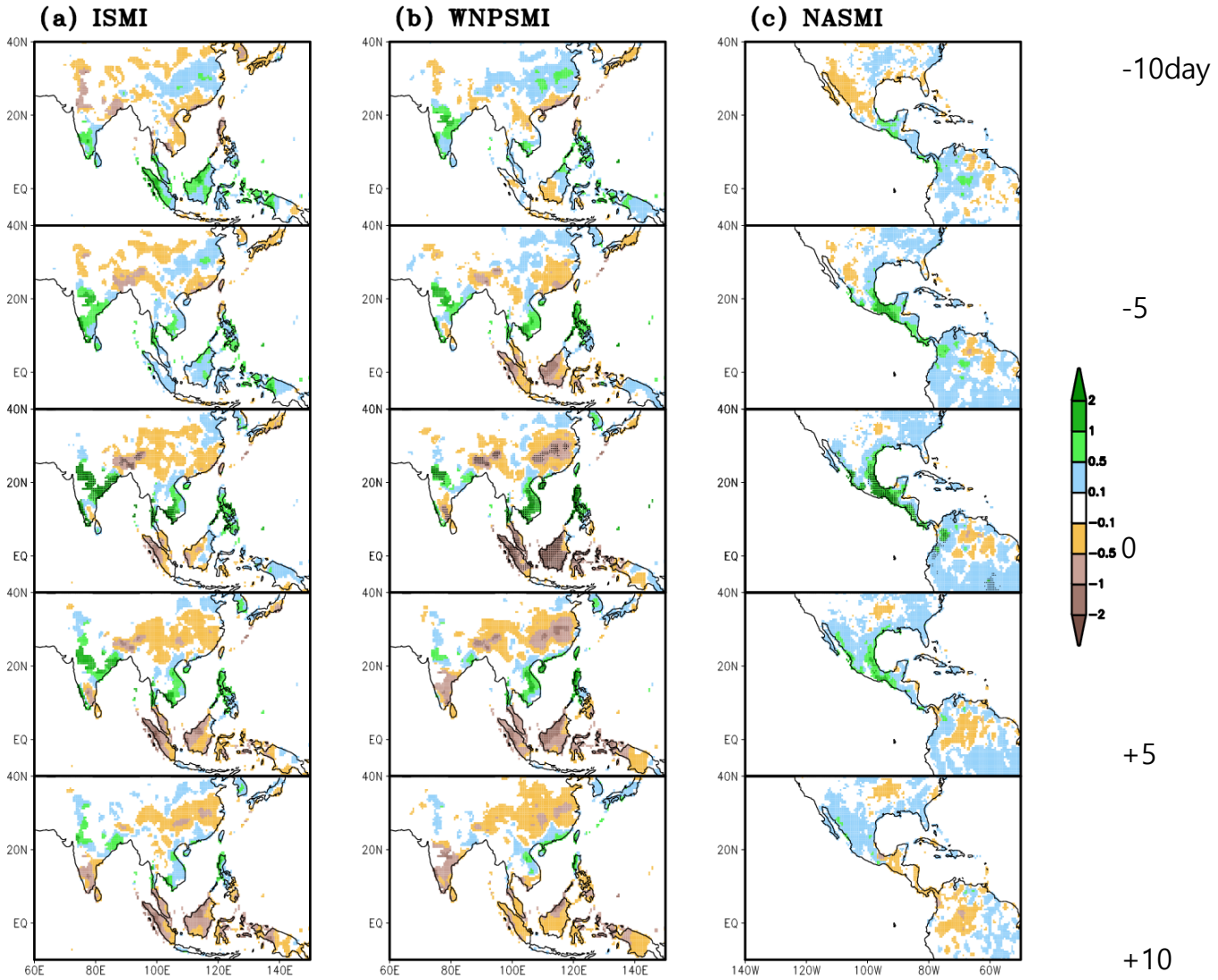

The intraseasonal precipitation anomalies over the Asian and American continents evolve in phase with the BSISO evolution

APCC APEC CLIMATE CENTER

Ref. Moon et al.

Teleconnection

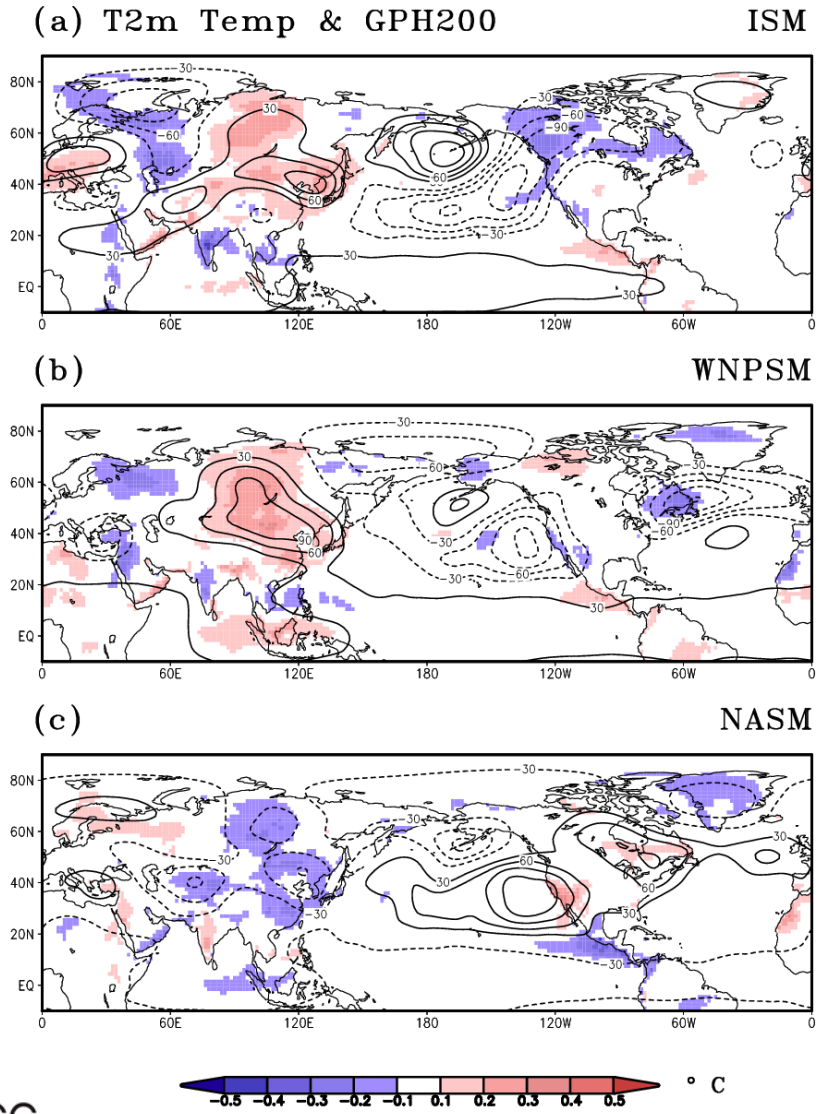

The surface air temperature anomaies highly correspond to the evolution of the BSISO teleconnection,

providing a source of intraseasonal predictability to extratropical regions.

APCC APEC CLIMATE CENTER

Ref. Moon et al.

Amplitude of two ISO modes: **Dec2009-Aug 2011**

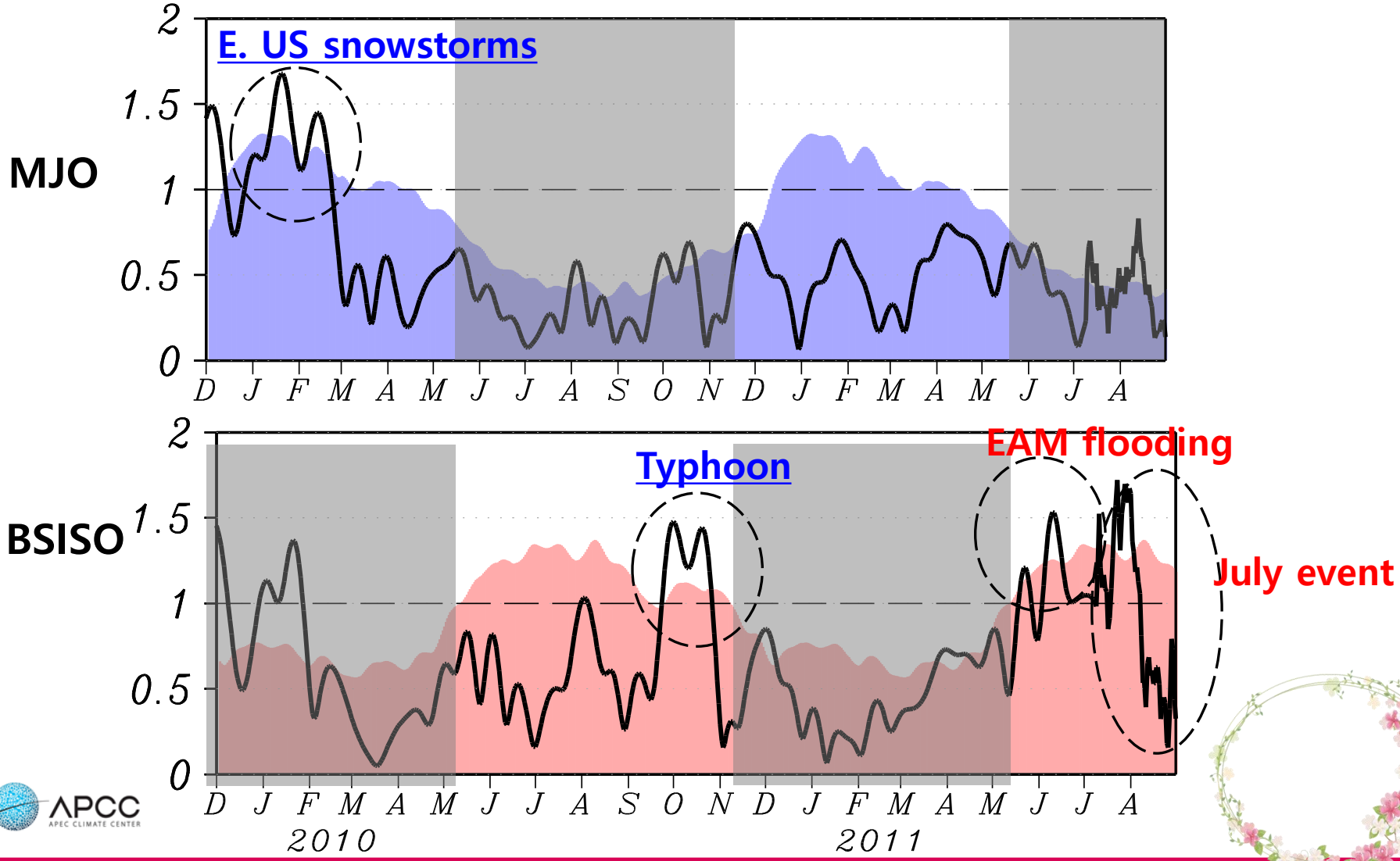

2009/10 snowstorms over eastern US

Ref. Moon et al.

MJO Modulation on 2009/10 Winter Snowstorms in the United States

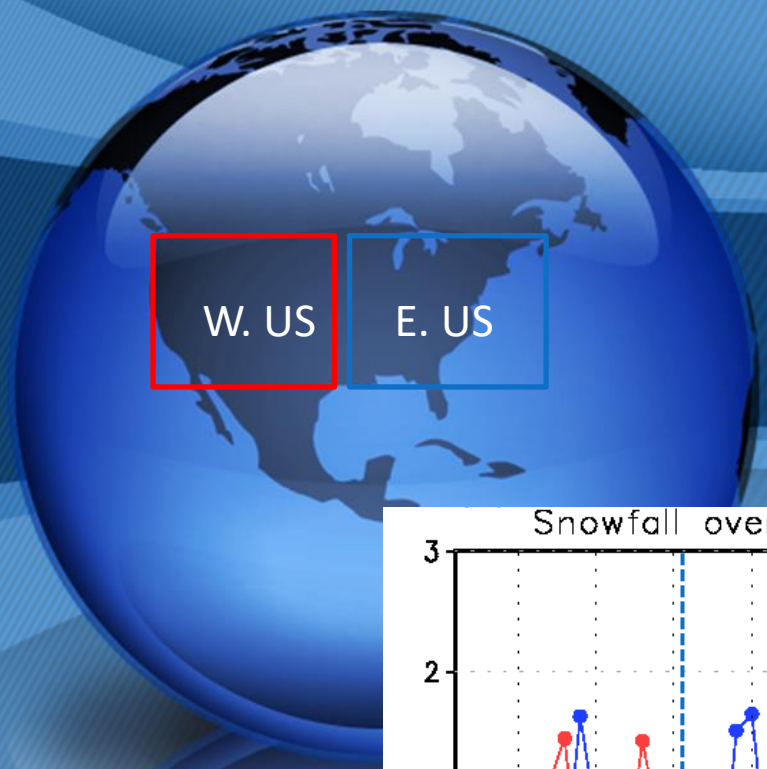

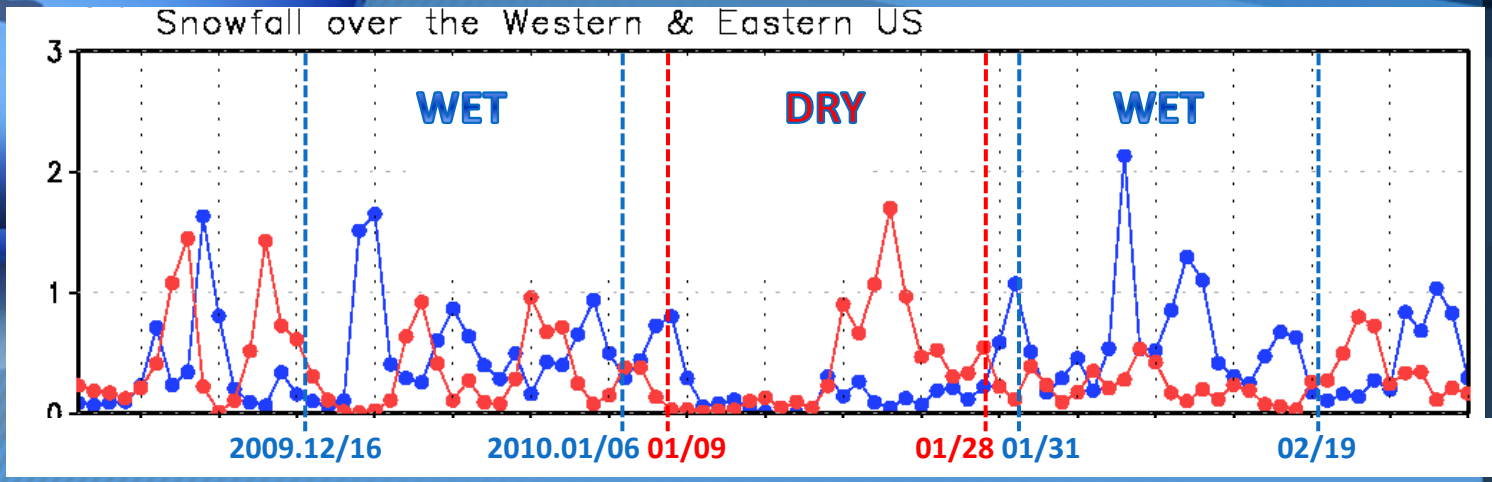

2009/10 Winter Snowstorm

- During the winter of 2009/10, heavy snowstorms dumped a tremendous amount of snow over the central to eastern parts of the US, with the largest amounts recorded over the Mid-Atlantic States.
- Snow cover for December in the contiguous US was the greatest ever recorded for that month.
- Two successive heavy snowstorms, which produced the highest amount of snowfall since the last century, occurred in early February, 2010: a massive snowstorm hit the US east coast and a huge and extremely dangerous snowstorm affected several Mid-Atlantic states, including North Carolina, Delaware, Washington, DC, Pennsylvania, Virginia, and Maryland.

- In the tropics, wet-dry-wet cycle of MJO over the central Pacific and Indian Ocean
- In the subtropics, this cycle lag behind the equatorial central Pacific (east of the dateline) by about 5-7 days

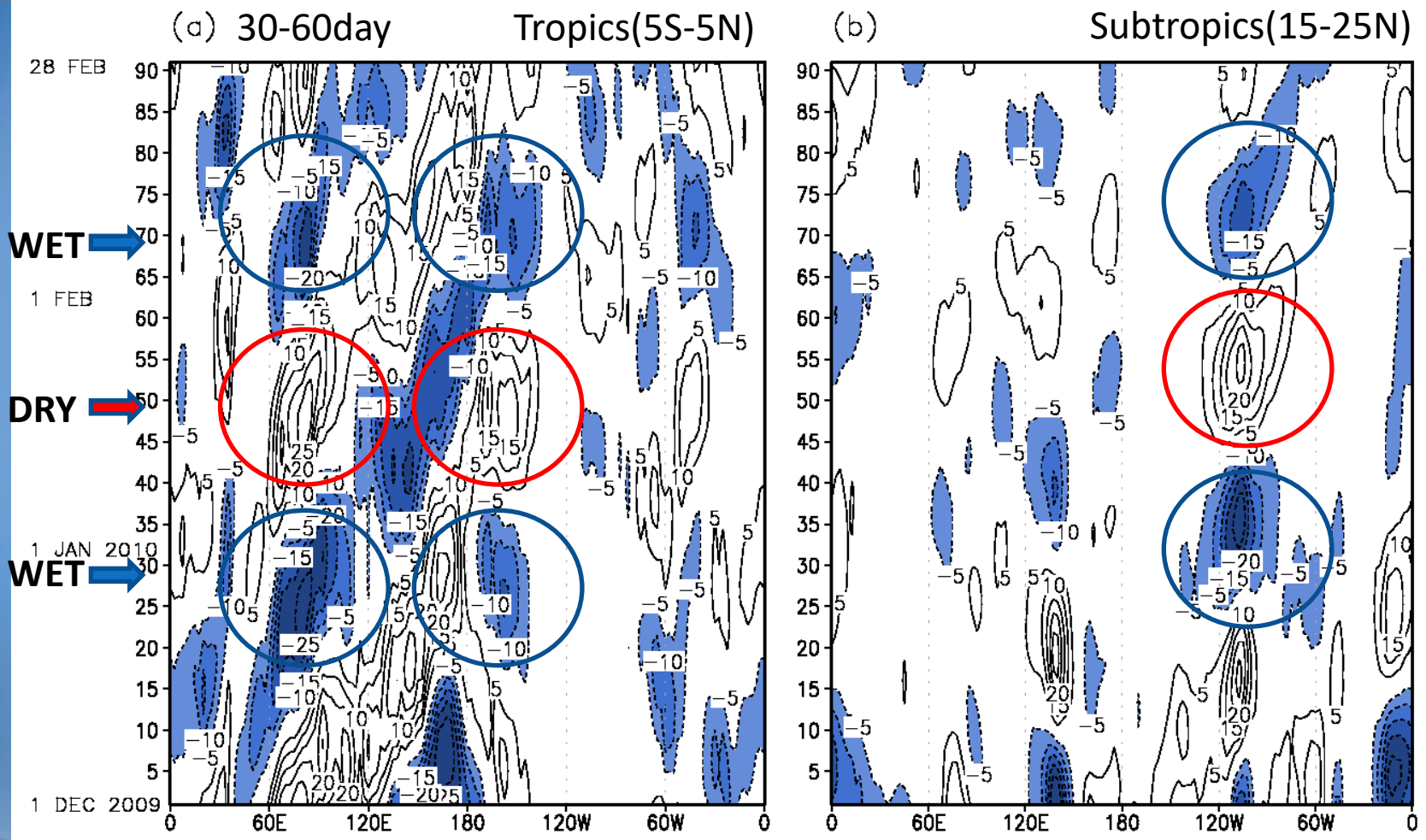

Intraseasonal anomalies of OLR and 300hPa streamfunction (left) 850hPa streamfunction and temperature (right) on the day of maximum convection over the tropical central Pacific from wet-dry-wet phase

Wet

Dry

Wet

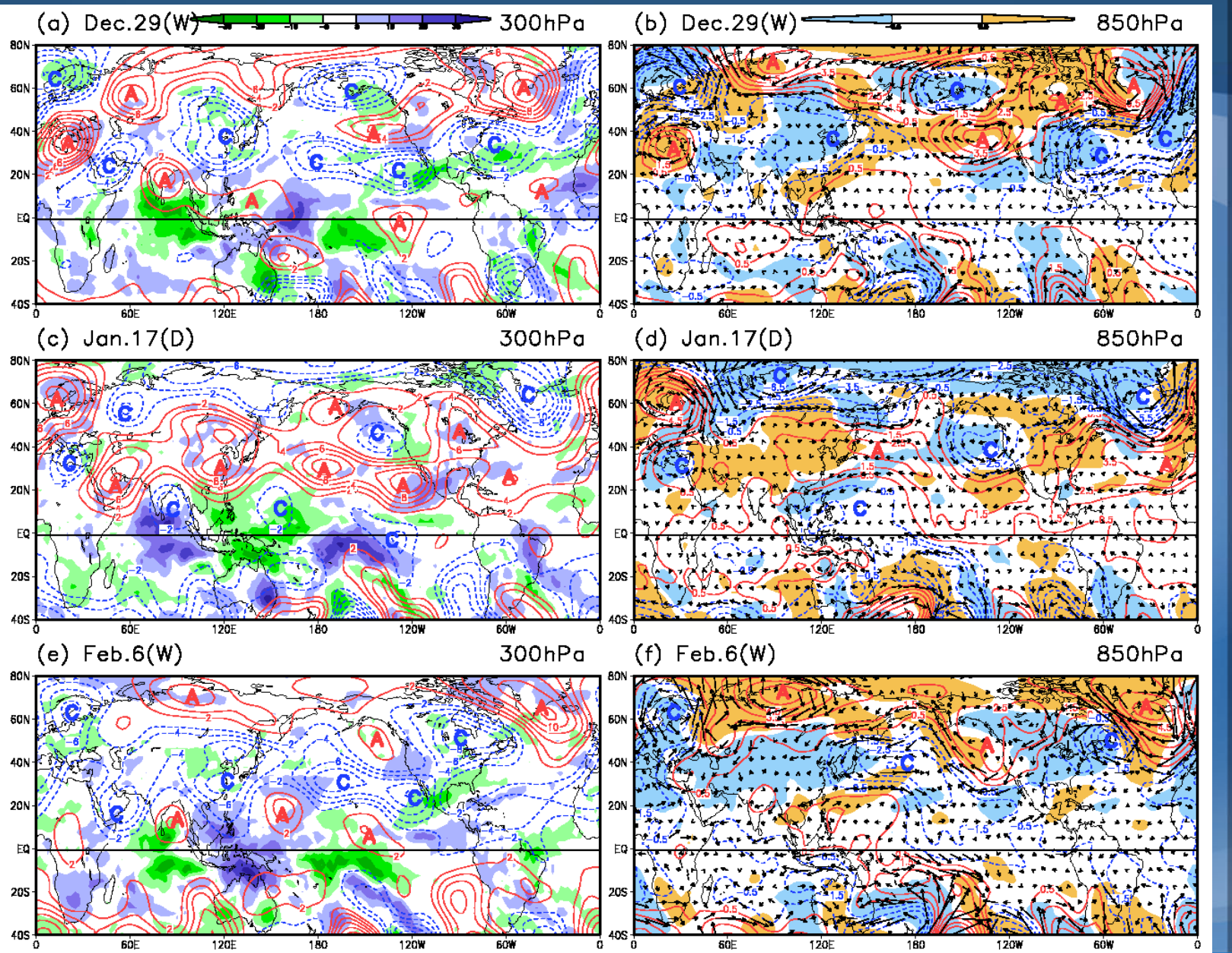

Fig. 1

Explanation of Fig

- The enhanced convection associated with MJO show two dominant areas over the tropical central Pacific and Indian Ocean. The enhanced convection is also seen from Mexico to the southern US. It is unusual that the MJO convection over the central Pacific maintains strength and extends toward Mexico-southern US when the ensuing MJO convection has already matured over the Indian Ocean.
- The upper- and lower-level circulations associated with the dry and wet episodes showed mirror-image patterns with the signs reversed, manifesting the obvious linkage of MJO modulation on the extratropics.

- In the wet episodes, a deep trough anchored over the central-eastern US and tilted westward with height. Hence, the low level had a dipole pattern of anticyclone (west) and cyclone (east), while the upper level maintained a cyclonic circulation over the entire US except for the western coast. As a result, the enhanced cold air from the high latitude penetrated southward and the central to eastern US was plunged into intense cold weather during the wet episodes.

Zonal vertical cross-sections of geopotential height (contour), temperature (shading), zonal wind and upward motion (vector) averaged between 30°N and 45°N.

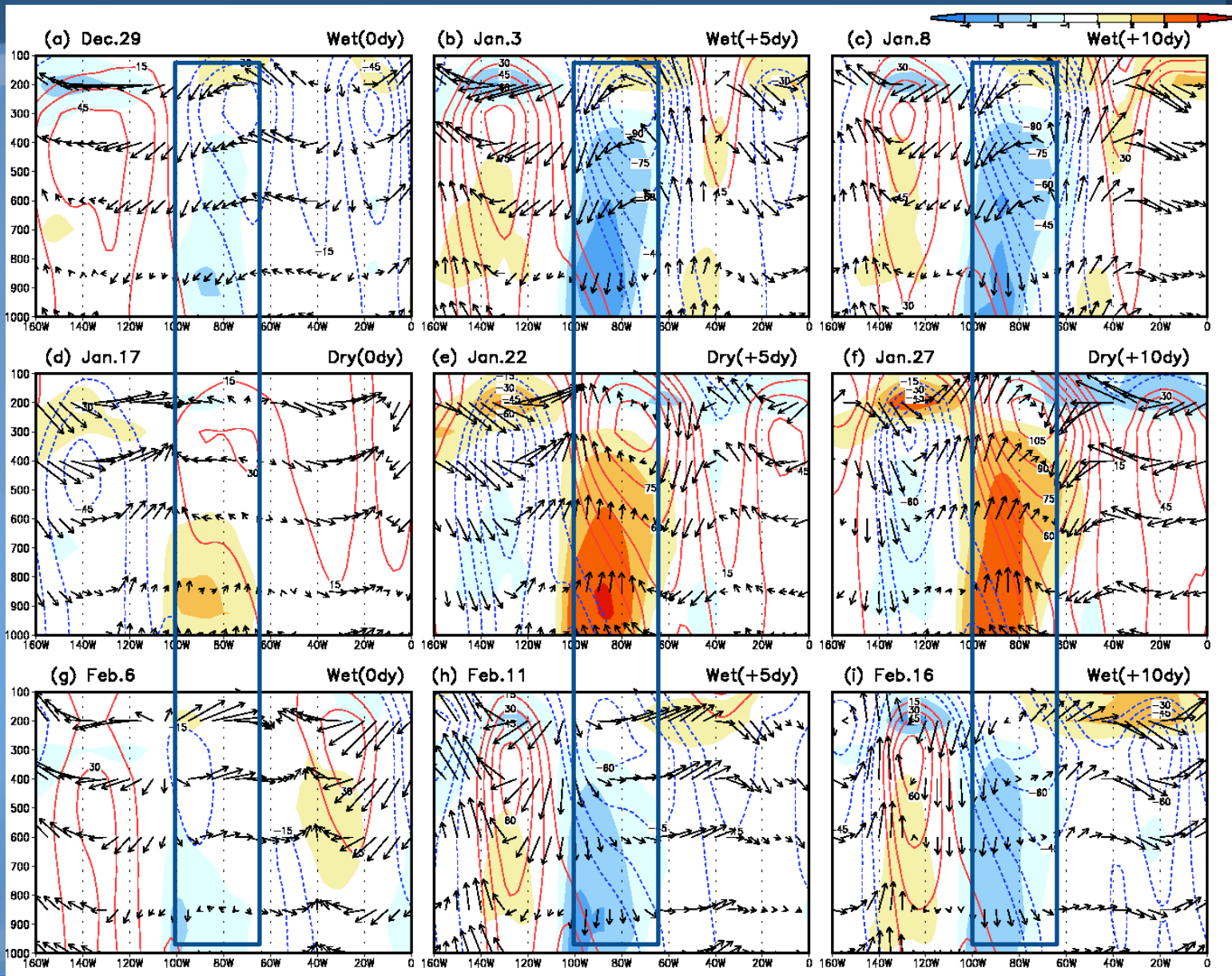

Fig. 2

Explanation of Fig

- During the wet episode, a deep ridge and a trough are found at day 0 in the western and eastern US, respectively.
- There is a descent in the eastern (western) part of the ridge (trough) and upward motion to the eastern side of the trough.
- In the low-level, the maximum cold temperature anomaly prevails at the descent area just beneath and to the left of the upper-level trough.
- The baroclinic disturbance developed over the central to eastern US with the minimum temperature.
- The synoptic disturbance occurring over the eastern US favored the development of severe snowstorms with the support of increased baroclinic instability due to warm and moist air confronting the cold air mass.

There is upward motion at the L sector and downward motion at the H sector during Feb.5~Feb.11.

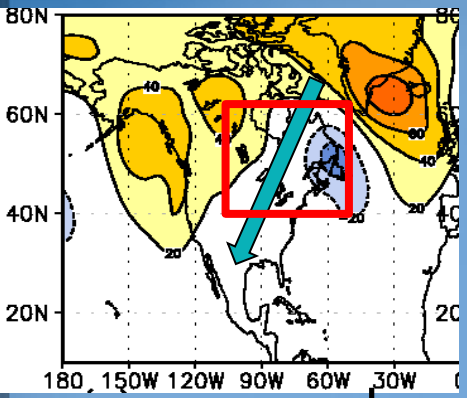

Along the arrow line, synoptic scale cyclone can be well-developed

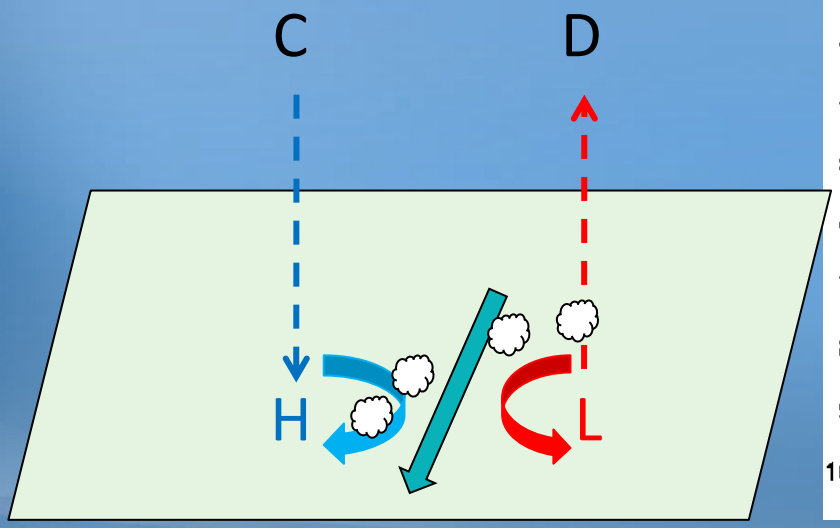

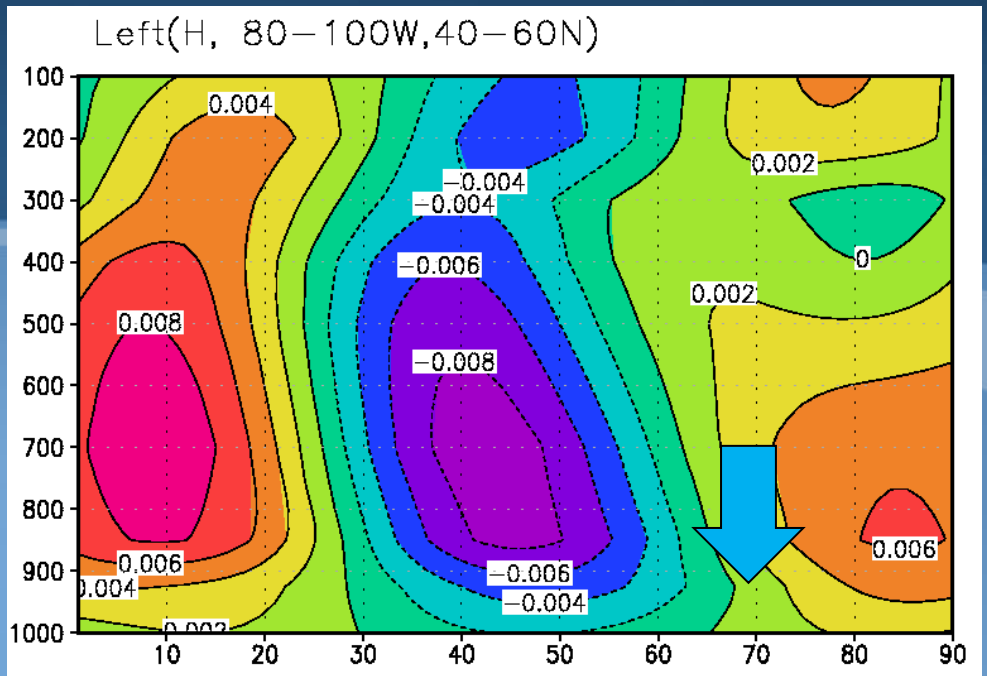

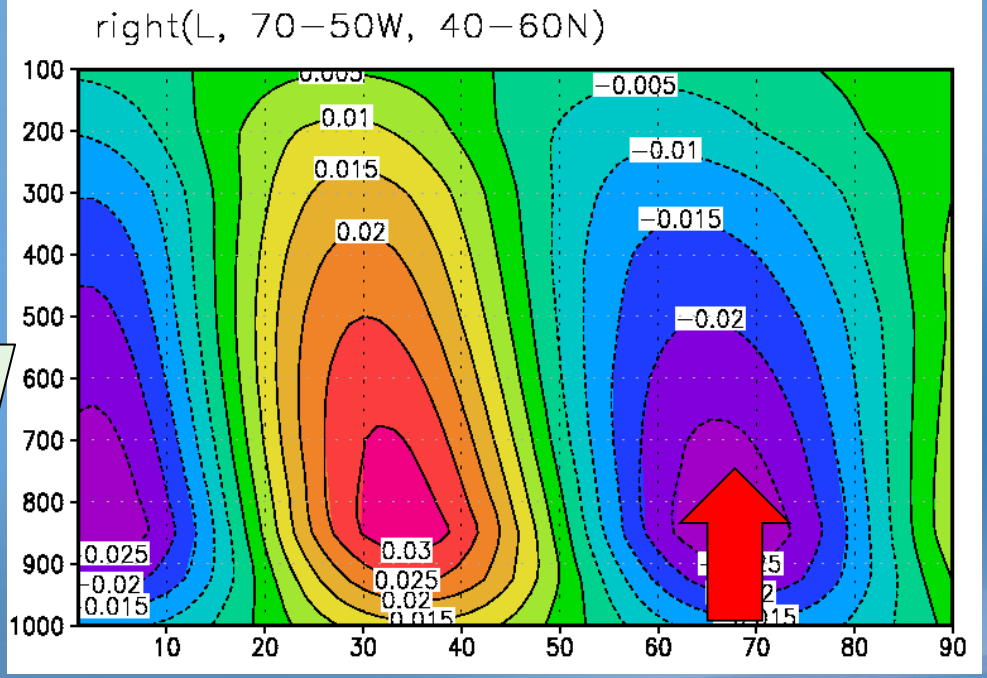

MJO impact on snowstorm

- During the winter of 2009/10, a number of record-breaking snowfall events registered in the eastern United States are shown to have been modulated by pulsation of tropical MJO through an atmospheric teleconnection pattern.
- From late December to mid-February, the convection over these two regions experienced a remarkable wet-dry-wet cycle; correspondingly, the daily snowfall over the eastern US also exhibited a wet-dry-wet cycle.
- As the MJO convection reached the central Pacific, a teleconnection pattern extends to North America, resulting in a westward-tilted deep anomalous trough anchored over the eastern US, producing a low-level pressure dipole anomaly with an anticyclone (cyclone) centered at the US west (east) coast.
- The enhanced high-latitude cold air penetrated southward, affecting the central and eastern US. Meanwhile, warm moist air was transported from the tropical central Pacific through Mexico to the southern US along with the upper-level subtropical westerly jet, which extended from the subtropical Pacific to the Atlantic Ocean. As such, the eastern US was located in a convergence zone between the enhanced cold air from the high-latitude and the warm moist air supplied from the subtropics, resulting in favorable condition for extremely heavy snowfall.

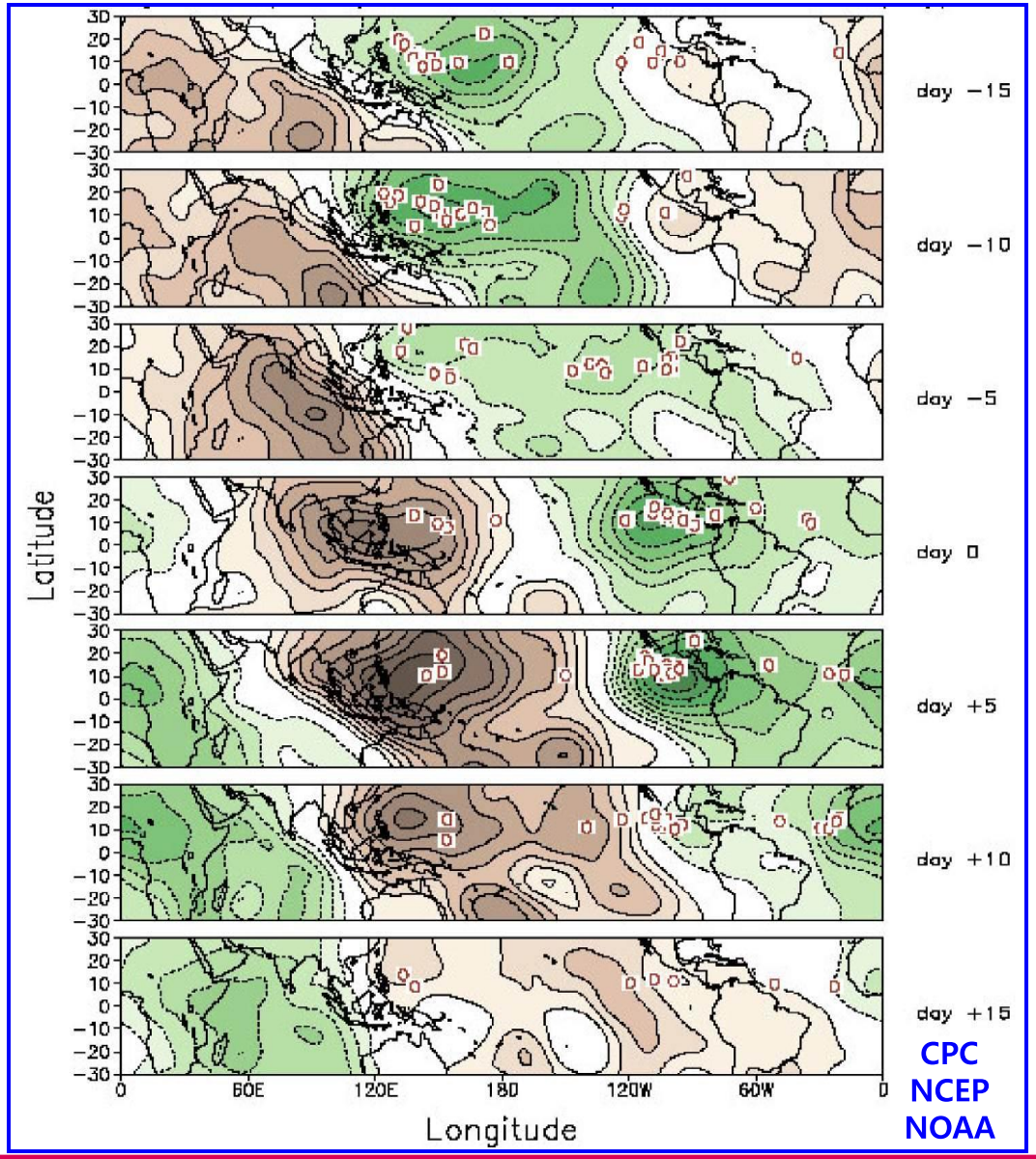

Remote Organization Of Tropical Cyclones

Higgins et al. 2000

The green (brown) shading roughly corresponds to regions where convection is favored (suppressed) as represented by 200-hPa velocity potential anomalies Composites are based on 21 events over a 35 day period. Hurricane track data is for the period JAS 1979-1997. Points of origin in each panel are for different storms. Contour interval is 0.5x106 m2 s-1, negative contours are dashed, and the zero contour is omitted for clarity.

Intraseasonal Variability at two different seasons

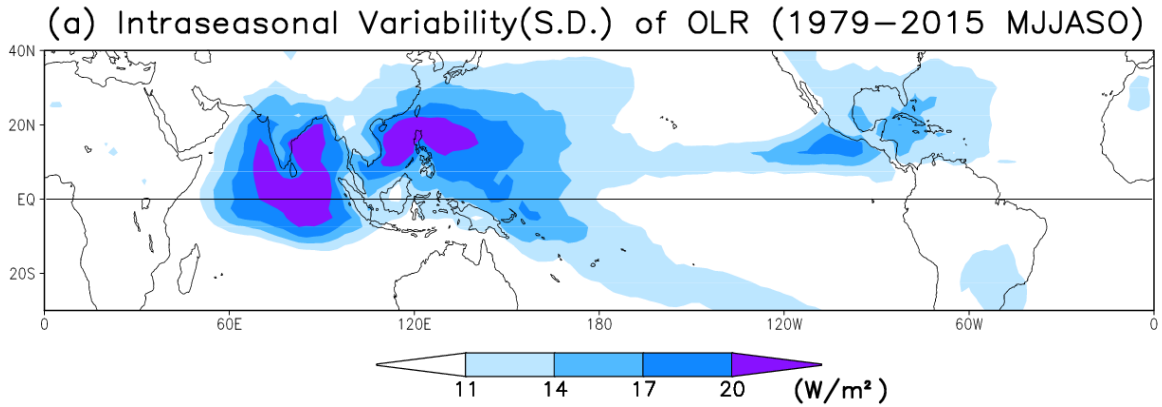

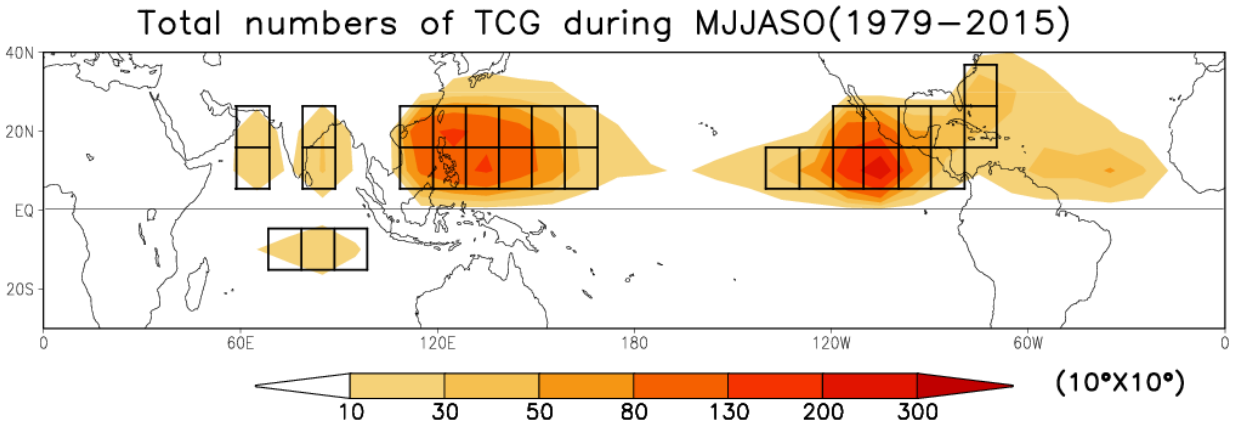

" During MJJASO, the major intraseasonal OLR variability is shifted to the NH mostly between the equator and 20°N "

"In NH summer (MJJASO), the TCG primarily occurs between 10°-20°N in the NH"

20-70day intraseasonal variability (standard deviation) of OLR during northern hemisphere summer (MJJASO) of 1979-2015 (top) and southern hemisphere summer (NDJFMA) of 1979-2014.

Total tropical cyclone genesis numbers at two different seasons

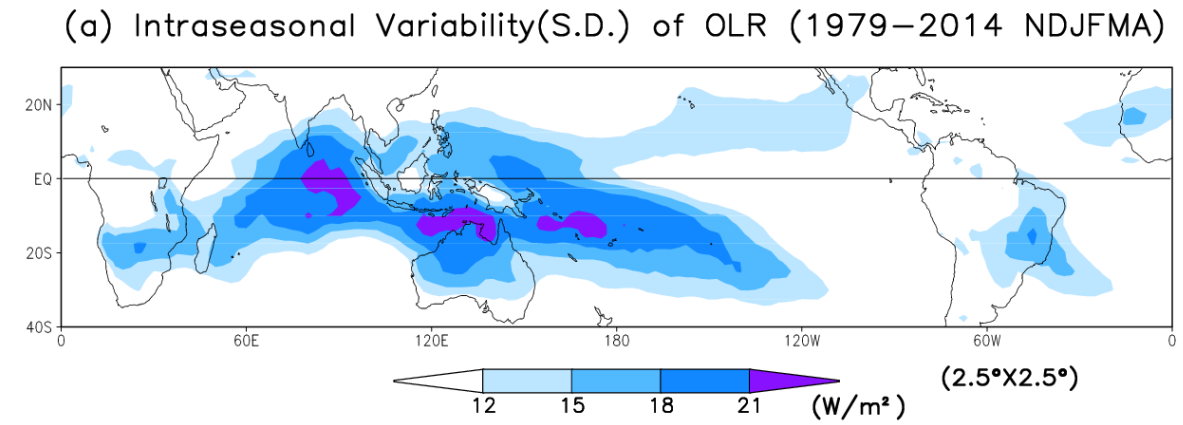

"In NDJFMA,
the major center shifts to
the SH mostly between
the equator and 20°S"

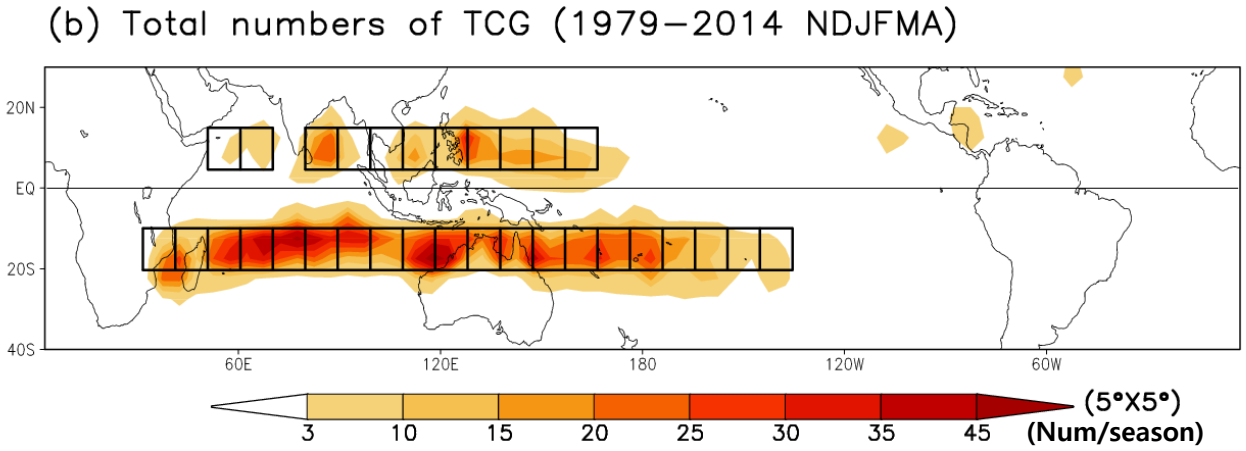

" In SH summer
(NDJFMA), the TCG
mainly
occurs between
10°-20°S in the SH "

Total numbers of tropical cyclone genesis during northern hemisphere summer (MJJASO) of 1979-2015 (top) and southern hemisphere summer (NDJFMA) of 1979-2014. Box indicates the selected 10°×10° locations of tropical cyclone genesis for stepwise regression analysis.

Teleconnection

BSISO_MJJASO

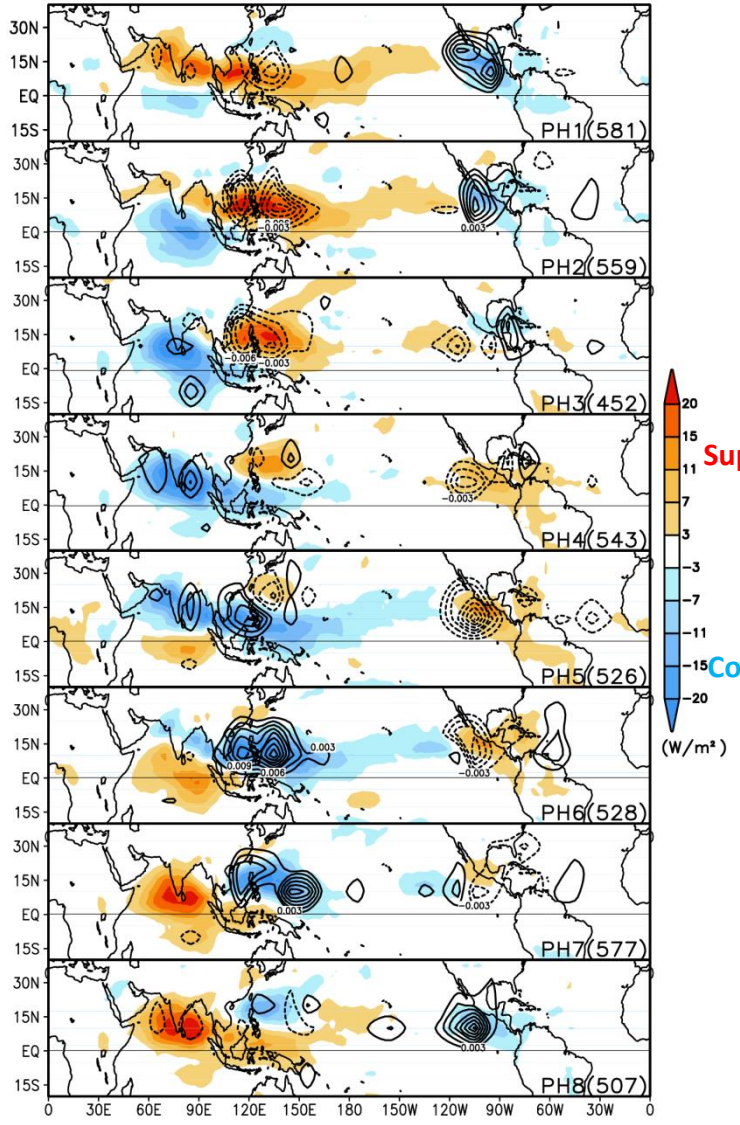

MJO_NDJFMA

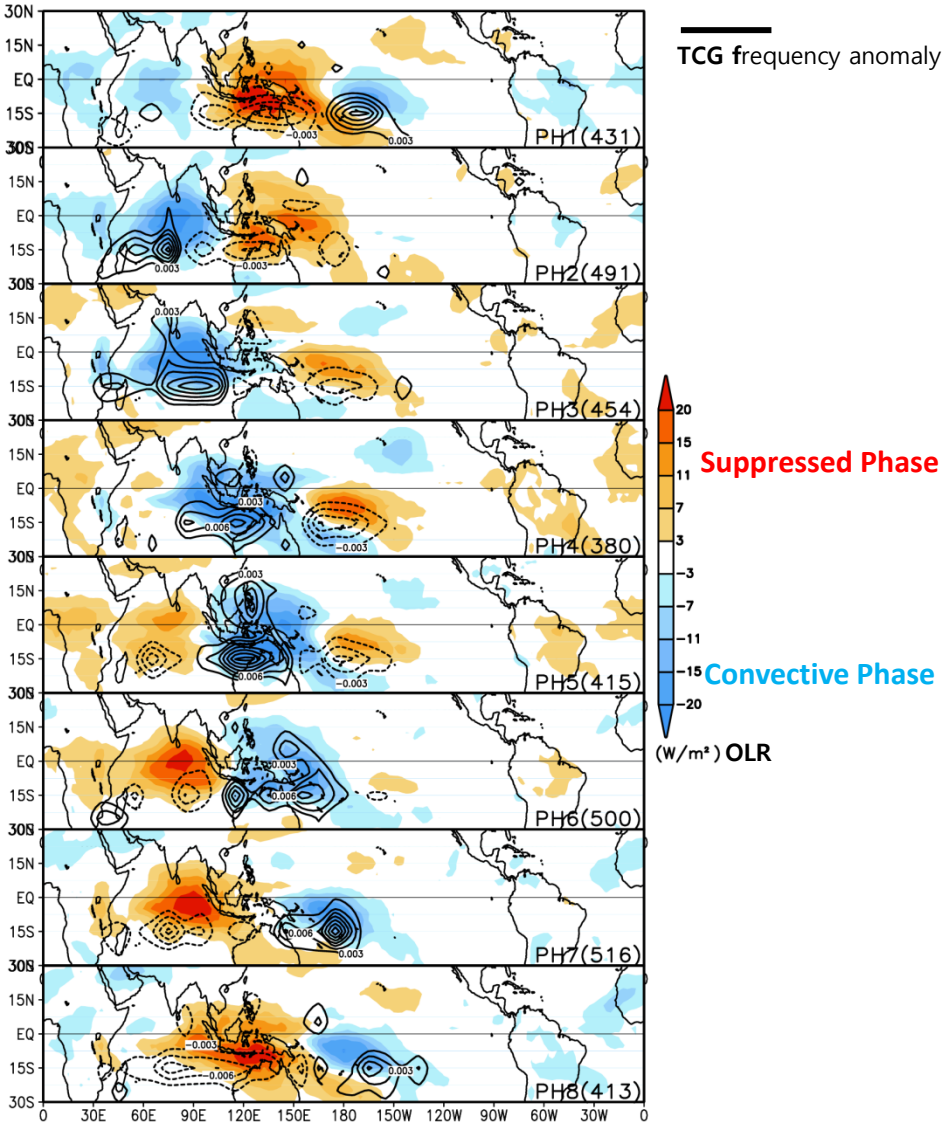

What are the MJO circulation factors regulating TCG potential

- Linking MJO circulation factors with TCG : Correlation table (248 samples)

(20S-EQ)	TCGF	V_{pot}	SST_a	RH_{600}	U_{x850}	U_{y500}	V_{zs}	V_s	$f\zeta_{r850}$	ω_{500}
TCGF	1.000	-0.275	-0.138	***0.553***	-0.254	***-0.539***	-0.418	-0.014	***0.726***	***-0.660***
V_{pot}	-0.275	1.000	0.473	0.035	-0.289	0.295	***0.713***	-0.014	***-0.533***	0.106
SST_a	-0.138	0.473	1.000	0.261	-0.422	0.423	0.351	-0.058	-0.388	-0.135
RH_{600}	***0.553***	0.035	0.261	1.000	***-0.747***	-0.177	-0.144	0.046	0.327	***-0.924***
U_{x850}	-0.254	-0.289	-0.422	***-0.747***	1.000	-0.080	-0.204	0.009	0.093	***0.659***
U_{y500}	***-0.539***	0.295	0.423	-0.177	-0.080	1.000	***0.510***	-0.061	***-0.802***	0.254
V_{zs}	0.418	***0.713***	0.351	-0.144	-0.204	***0.510***	1.000	-0.028	***-0.748***	0.260
V_s	-0.014	-0.014	-0.058	0.046	0.009	-0.061	-0.028	1.000	0.029	-0.005
$f\zeta_{r850}$	***0.726***	***-0.533***	-0.388	0.327	0.093	***-0.802***	***-0.748***	0.029	1.000	***-0.503***
ω_{500}	***-0.660***	0.106	-0.135	***-0.924***	***0.659***	0.254	0.260	-0.005	***-0.503***	1.000

The bold numbers indicate correlation coefficient greater than 0.5.

- Highest correlation is $f\zeta_{r850}$ and the second highest is ω_{500}
- The vertical shear Vs and MPI V_{pot} are not important!
- RH_{600} is the best among ENGPI factors but highly related to ω_{500} (r=-0.92)
- Vertical shear of zonal winds is better than the total vertical wind shear

Table Correlation coefficient s table among 9 candidate factors and the tropical cyclone genesis frequency as well as between two candidate factors. The italic-bold numbers indicate absolute value is greater than 0.5. Sample size is 248.

Modulation of Tropical Cyclone Genesis by MJO at three hot spots over the SH Ocean

Ref. Wang and Moon

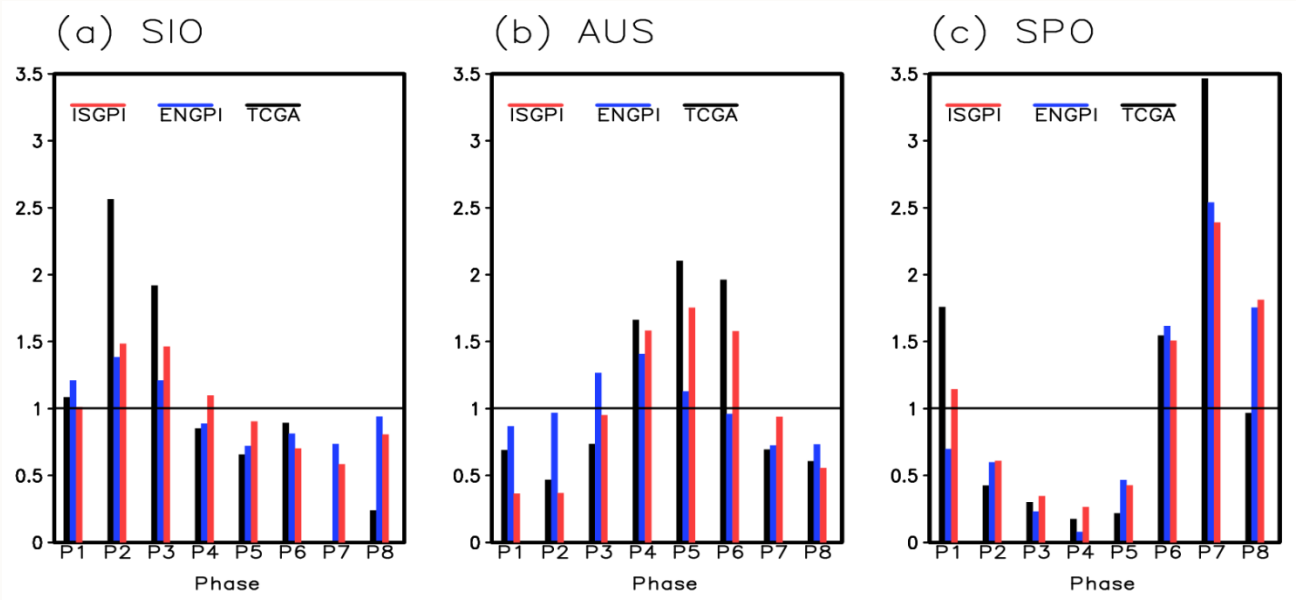

The normalized TCG frequency (by its corresponding climatological mean TCG frequency) derived from observation (black bar) and predicted by ISGPI (red bar) and ENGPI (blue bar) at three hot spots of TCG zone in the Southern Hemisphere: (a) southern Indian Ocean (SIO, 70°-80°E, 10°-20°S), (b) Australia region (AUS, 110°-120°E, 10°-20°S), and (c) South Pacific Ocean (SPO, 170°E-180°, 10°-20°S) during composite eight phases (P1 to P8) of MJO in austral summer (NDJFMA) of 1979~2014.

- **Near the dateline in SPO, the probability of TCG at the wettest phase is 3.5 times of the climatological value while in the driest phase it decreases to 20% of the climatological value.**
- **The ratio of TCG probability between the wettest and driest phases of MJO is 19 at SPO. Similarly, this ratio is 11 at SIO, and 5 over the northwest of Australia.**
- **These remarkable modulations are captured quite well by the ISGPI.**

=> If dynamical model can faithfully predict large scale anomalies, *Application of the new ISGPI may have a large potential to improve sub-seasonal prediction of TC genesis.*

What are the BSISO circulation factors regulating TCG potential

- Linking BSISO circulation factors with TCG : Correlation table (248 samples)

(EQ-20°N)	$TCGF$	V_{pot}	η_{850}	RH_{600}	V_s	SST_a	U_{x850}	U_{y500}	V_{zs}	$f\zeta_{r850}$	ω_{500}
$TCGF$	**1.00**	-0.15	**0.61**	**0.61**	-0.10	**-0.22**	**-0.45**	**-0.60**	**-0.38**	**0.60**	**-0.68**
V_{pot}	-0.15	**1.00**	**-0.22**	-0.01	-0.05	**0.72**	-0.17	**0.24**	**0.49**	**-0.34**	0.01
η_{850}	**0.61**	-0.22	**1.00**	**0.69**	-0.07	-0.13	**-0.39**	**-0.86**	**-0.22**	**0.97**	**-0.74**
RH_{600}	**0.61**	-0.01	**0.69**	**1.00**	-0.05	**-0.18**	**-0.68**	**-0.63**	**-0.26**	**0.61**	**-0.94**
V_s	-0.10	-0.05	-0.07	-0.05	**1.00**	0.03	0.06	0.03	0.03	-0.06	0.04
SST_a	**-0.22**	**0.72**	-0.13	**-0.18**	0.03	**1.00**	0.08	0.11	**0.56**	**-0.24**	0.16
U_{x850}	**-0.45**	-0.17	**-0.39**	**-0.68**	0.06	0.08	**1.00**	**0.31**	0.10	**-0.27**	**0.68**
U_{y500}	**-0.60**	**0.24**	**-0.86**	**-0.63**	0.03	0.11	**0.31**	**1.00**	**0.33**	**-0.84**	**0.69**
V_{zs}	**-0.38**	**0.49**	**-0.22**	**-0.26**	0.03	**0.56**	0.10	**0.33**	**1.00**	**-0.30**	**0.21**
$f\zeta_{r850}$	**0.60**	**-0.34**	**0.97**	**0.61**	-0.06	**-0.24**	**-0.27**	**-0.84**	**-0.30**	**1.00**	**-0.66**
ω_{500}	**-0.68**	0.01	**-0.74**	**-0.94**	0.04	0.16	**0.68**	**0.69**	**0.21**	**-0.66**	**1.00**

The bold numbers indicate statistically significant at 95% confidence level.

- ω_{500} (r=-0.92) has the highest correlation.
- The vertical shear V_s and MPI V_{pot} , and SST_a are the lowest.
- RH_{600} and η_{850} are closely related to ω_{500} (r=-0.94 and r=-0.74).
- $f\zeta_{r850}$ and V_{zs} have significant correlations with TCGF and physically more independent feature with ω_{500}.

Table Correlation coefficients table among 10 candidate factors and the tropical cyclone genesis frequency (TCGF) as well as between each of the two candidate factors. The bold numbers indicate statistically significant at 95% confidence level. Sample size is 248.

Modulation of Tropical Cyclone Genesis by BSISO over the NH Ocean

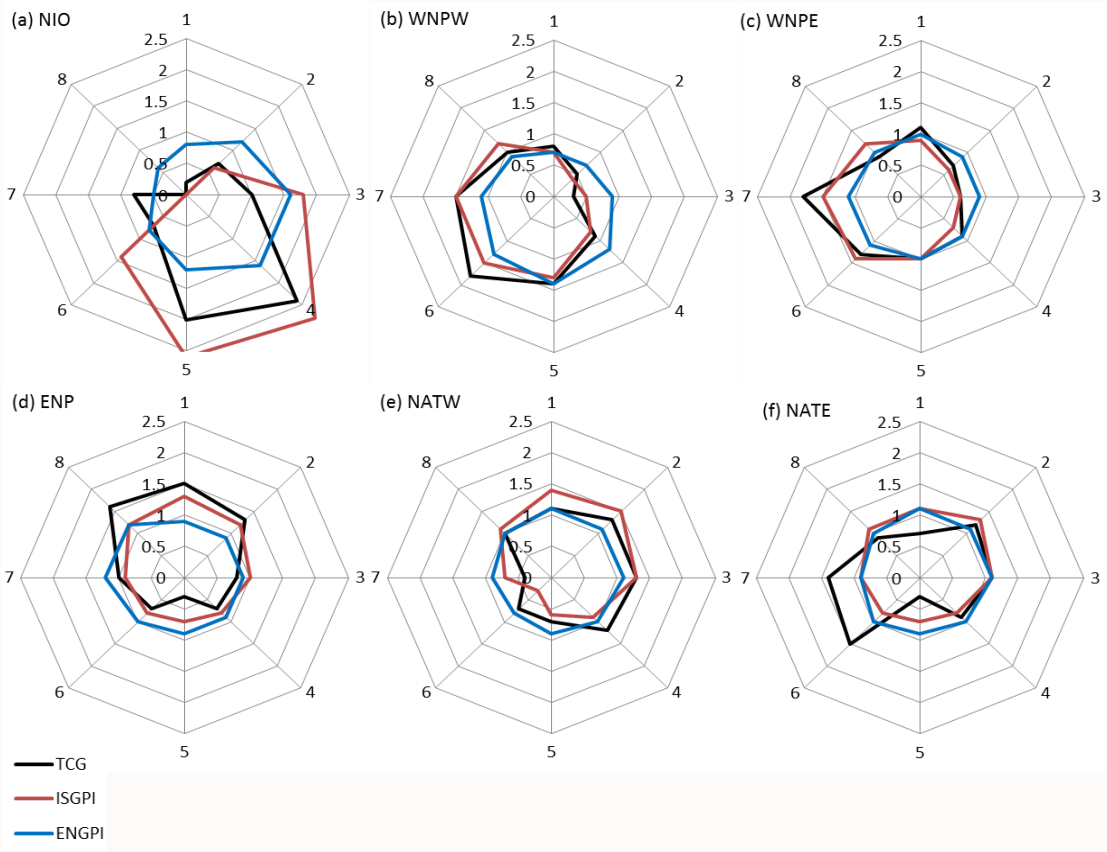

- **The probability of TCG at each sub-region significantly increases at the BSISO convective phase compared to its suppressed phase: At Phases 4-5 in NIO, Phases 5-7 in WNPW, Phases 6-7 in WNPE, Phases 8-2 in ENP, Phases 1-4 in NATW, and Phase 2-3 and 6-7 in NATE.**
- **The ratio of TCG probability between the convective and suppressed phase of BSISO is 12 at NIO, 6 at WNPW, 3 at WNPE, 5 at ENP, 3 at NATW, and 5 at NATE.**
- **The BSISO control on TCG probability is better detected in ISGPI than the ENGPI, as evidenced by a close match of the red (ISGPI) and black (TCG) curves, suggesting that the probabilistic prediction of TCG can be improved by using ISGPI.**

The normalized TCG frequency (by its corresponding climatological mean TCG frequency at each sub-region) during composite eight phases (1 to 8) of BSISO in NH summer. Results are derived from observation (black) and predicted by ISGPI (red) and ENGPI (blue) at six TCG zones in the Northern Ocean: (a) NIO, (b) WNPW, (c) WNPE, (d) ENP, (e) NATW, and (f) NATE.


Q & A

Thank you